Geofluids (2001) **1**, 11–36

Interpretation of observed fluid potential patterns in a deep sedimentary basin under tectonic compression: Hungarian Great Plain, Pannonian Basin

J. TÓTH AND I. ALMÁSI

Department of Earth and Atmospheric Sciences, University of Alberta, Edmonton, Alberta, Canada

ABSTRACT

The $\approx$ 40 000 km^2 Hungarian Great Plain portion of the Pannonian Basin consists of a basin fill of 100 m to more than 7000 m thick semi- to unconsolidated marine, deltaic, lacustrine and fluviatile clastic sediments of Neogene age, resting on a strongly tectonized Pre–Neogene basement of horst–and–graben topography of a relief in excess of 5000 m. The basement is built of a great variety of brittle rocks, including flysch, carbonates and metamorphics. The relatively continuous Endrőd Aquitard, with a permeability of less than 1 md (10^{-15} m^2) and a depth varying between 500 and 5000 m, divides the basin's rock framework into upper and lower sequences of highly permeable rock units, whose permeabilities range from a few tens to several thousands of millidarcy. Subsurface fluid potential and flow fields were inferred from 16 192 water level and pore pressure measurements using three methods of representation: pressure–elevation profiles; hydraulic head maps; and hydraulic cross-sections.

Pressure–elevation profiles were constructed for eight areas. Typically, they start from the surface with a straight-line segment of a hydrostatic gradient (γ_{st} = 9.8067 MPa km^{-1}) and extend to depths of 1400–2500 m. At high surface elevations, the gradient is slightly smaller than hydrostatic, while at low elevations it is slightly greater. At greater depths, both the pressures and their vertical gradients are uniformly superhydrostatic. The transition to the overpressured depths may be gradual, with a gradient of γ_{dyn} = 10–15 MPa km^{-1} over a vertical distance of 400–1000 m, or abrupt, with a pressure jump of up to 10 MPa km^{-1} over less than 100 m and a gradient of γ_{dyn} > 20 MPa km^{-1}.

According to the hydraulic head maps for 13 100–500 m thick horizontal slices of the rock framework, the fluid potential in the near-surface domains declines with depth beneath positive topographic features, but it increases beneath depressions. The approximate boundary between these hydraulically contrasting regions is the 100 m elevation contour line in the Duna–Tisza interfluve, and the 100–110 m contours in the Nyírség uplands. Below depths of $\approx$ 600 m, islets of superhydrostatic heads develop which grow in number, areal extent and height as the depth increases; hydraulic heads may exceed 3000 m locally. A hydraulic head 'escarpment' appears gradually in the elevation range of $-$ 1000 to $-$ 2800 m along an arcuate line which tracks a major regional fault zone striking NE–SW: heads drop stepwise by several hundred metres, at places 2000 m, from its north and west sides to the south and east. The escarpment forms a 'fluid potential bank' between a 'fluid potential highland' (500–2500 m) to the north and west, and a 'fluid potential basin' (100–500 m) to the south and east. A 'potential island' rises 1000 m high above this basin further south.

According to four vertical hydraulic sections, groundwater flow is controlled by the topography in the upper 200–1700 m of the basin; the driving force is orientated downwards beneath the highlands and upwards beneath the lowlands. However, it is directed uniformly upwards at greater depths. The transition between the two regimes may be gradual or abrupt, as indicated by wide or dense spacing of the hydraulic head contours, respectively. Pressure 'plumes' or 'ridges' may protrude to shallow depths along faults originating in the basement. The basement horsts appear to be overpressured relative to the intervening grabens.

The principal thesis of this paper is that the two main driving forces of fluid flow in the basin are gravitation, due to elevation differences of the topographic relief, and tectonic compression. The flow field is unconfined in the gravitational regime, whereas it is confined in the compressional regime. The nature and geometry of the fluid potential field between the two regimes are controlled by the sedimentary and structural features of the rock units in that domain, characterized by highly permeable and localized sedimentary windows, conductive faults and fracture zones. The transition between the two potential fields can be gradual or abrupt in the vertical, and island-like or ridge-like in plan view. The depth of the boundary zone can vary between 400 and 2000 m. Recharge to the gravitational regime is

inferred to occur from infiltrating precipitation water, whereas that to the confined regime is from pore volume reduction due to the basement's tectonic compression.

Key-words: gravity flow systems, Hungarian Great Plain, Pannonian Basin, subsurface hydraulics, tectonic compression

Received 20 April 2000; accepted 16 October 2000

Corresponding author: József Tóth, Department of Earth and Atmospheric Sciences, University of Alberta, Edmonton, Alta, T6G 2E3, Canada.

Geofluids (2001) **1**, 11-36

INTRODUCTION

The Pannonian Basin in general, and the Great Plain of Hungary in particular, have long been the subjects of intensive geoscience research, such as structural geology, geophysics, petroleum geology and hydrogeology (Ballentine *et al.* 1991; Clayton *et al.* 1990; Dobos 1985; Erdélyi 1976; Hungarian Geological Survey 1993; Royden & Horváth 1988). As a result of these interests, large databases related to petroleum exploration and groundwater resources are available. Remarkably, however, these separate databases have never been merged or used in combination to produce a comprehensive hydrogeological evaluation of the basin, although numerous studies have been conducted on a great variety of specific hydrogeologically related problems.

The purpose of this paper is to present our understanding of the basic hydrogeological conditions and their causes in the Hungarian Great Plain portion of the Pannonian Basin. Thus the central objective of this study is to describe and interpret the fluid potential distribution of the basin's formation waters, making use of the relevant components of both databases. Such characterization allows inferences to be made regarding the origin of fluid driving forces, regional patterns of subsurface water flow, relative amounts of water derived from possibly different sources and the principal controls on the flow geometry, including structural or sedimentological discontinuities.

DATABASE

The major types of basic data used in the study are geodetical, geological, rock physical and fluid dynamic. Part of this information was obtained in the form of original measurements or processed data from the databanks of various Hungarian industrial firms, government departments and research organizations, while other information was obtained as in-house reports, conference proceedings, published papers and monographs. Owing to the large volume, great diversity, different forms and variable quality of the information, it was necessary to cull, consolidate and normalize the data, and to establish a database specifically for the present purposes. Particular effort was made therefore to compile a dataset from the existing measurements of formation pressures and water levels, which is as complete and as rigorously screened as possible.

All geodetic information is expressed in the Hungarian 'EOV' coordinate system (EOV = Egységes Országos Vetületi rendszer = Uniform National Projection system). The system uses the horizontal Y_{EOV}- and X_{EOV}-plane coordinate axes to express, respectively, the Easting and Northing distances, in metres, from the system's origin. The origin is located outside the country to the south–west so as to make all possible EOV coordinates positive in Hungary. Elevations are measured on the vertical Z_{EOV}-axis and referenced to Baltic sea level, with the sense being positive upwards.

The description of the rock framework is based on stratigraphic, lithologic and rock physical data from 1274 bore holes, many of which were drilled hundreds of metres into the Pre-Neogene basement; numerous in-house reports and published papers; and published data and maps on structure and tectonic history. The resolution of the obtained image is adequate for the regional portrayal of the rock framework, but is insufficient for local analyses.

A grand total of nearly 53 000 pore pressure and water level measurements were collected. Pore pressure data were obtained from petroleum exploration activities in the form of either original 'Drill–Stem–Test' (DST) pressure build-up charts or already calculated initial formation pressures. These data cover mainly the deeper zones of the basin, i.e. below approximately 600–800 m. Nonpumping and production water levels are largely derived from water supply developments. The sources of these data include bored and hand-dug water table wells a few metres deep, drilled municipal and industrial water wells reaching to depths of 1000–1500 m, and still deeper thermal wells used for health spas and heating of green houses and apartment buildings. Many of the obtained records lacked essential data or were otherwise deficient, such as: incomplete sets of position coordinates; missing drilling fluid densities; no timing, duration and/or rate of fluid production; and so on. Ultimately, 1294 of 3706 (or 34.9%) DST pressure measurements and 14 898 of 49 265 (or 30.2%) water level measurements have been retained

and incorporated into the study's database to yield a total of 16 192 hydraulic head values out of a total of 52 971 records.

THE STUDY AREA

With its approximately 40 000 km^2, the study area covers most of the Hungarian Great Plain region of the Pannonian Basin in Central Europe (Fig. 1). The basin is a major, near-circular intermontane depression of about 500 km in diameter. It is almost completely surrounded by a belt of high mountains comprising the Alps, the Carpathians and the Dinarides. The highest peaks of all these ranges rise above 2500 m, while their average elevations are ≈ 2000 m, ≈ 1500 m and ≈ 1000 m, respectively.

The Great Plain is bounded by the Duna River to the west; the foothills of the Hungarian North Central Range, which is the central front range of the Carpathians, to the north; and by the international boundaries with Slovakia, the Ukraine, Romania and Serbia, respectively, to the north, north–east, south–east and south (Fig. 2). The maps, cross–sections and observation points of the study are referenced to a rectangular base map prepared for the present purpose with the following corner points (and side lengths) in the 'EOV' coordinate system: X_{EOV} = from 60 km to 360 km (300 km) and Y_{EOV} = from 620 km to 940 km (320 km).

The area is well drained, primarily by the Tisza River and its tributaries (Fig. 2). The Tisza enters the area in the north–east and leaves across the centre of its south boundary. The main tributaries, the Zagyva, the Körös River sytem and the Maros, flow over the lowest part of the study area, namely the extensive and flat central depression of the Great Plain. The topographic elevation of this plane surface varies between approximately 80 and 90 m above sea level (a.s.l.). The other, much smaller, flat and low–lying region is a 5–25 km wide strip of land stretching along the left bank of the Duna River, where topographic elevations vary between 90 and 95 m. These two principal depressions are bordered by areally extensive, but only moderately elevated, highlands. Most notable of these hydrogeologically important morphologic features are the WSW–ENE-striking hills along the base of the North Central Range, with elevations reaching 400–600 m; the broad ridge along the N–S–orientated axis of the Duna–Tisza interfluve, with elevations exceeding 200 m in the Gödöllő Hills at the interfluve's north end, and 140 m at Illancs, in the south; and the broad sandy hills of the Nyírség, in the north–east, rising over 160 m. Within distances of 60–100 km to the east and south of the area's eastern and southern boundaries, the Apuseni mountains and the Dinarides complete the circle of high ground around the entire area (Fig. 1). Breaking the continuity of the high topography are the strips of lowlands where the major rivers enter and exit from the area.

Fig. 1. Location of the Pannonian Basin and the Great Plain of Hungary in the regional context.

Geologically, the Pannonian Basin is a complex sedimentary basin which comprises a number of deep local basins, such as the Vienna Basin, the Little Plain of Hungary and several deep troughs beneath the Great Plain. In the study area, a 100 m to more than 7000 m thick semi- to unconsolidated clastic basin fill of marine, deltaic, lacustrine, fluviatile and eolian strata of Neogene age rest on a Pre–Neogene basement of brittle flysch, carbonate and metamorphic rocks of a high-relief horst-and-graben topography.

Neogene sedimentation started with general rifting and rapid subsidence in Early Miocene times (19 Ma) with the deposition of clays, conglomerates and, locally, coals of the Karpatian Formation (Fig. 3). Extension and rifting continued throughout the Middle Miocene (16.5–11.5 Ma), resulting in thick deposits of marine sediments, such as limestones, marls and turbidites, forming the Badenian and Sarmatian Formations. At the end of the rifting period, the morphology of the basin's surface was one of high relief due to variable amounts of extension, uplift and subsidence in different regions. Islands of older rocks alternated with deep troughs filled with thousands of metres of syn-rift deposits. High- and low-angle normal faulting, tectonic unroofing and transfer faults gave rise to complex systems of rock framework discontinuities and a basin–and–range morphology by the end of the Middle Miocene (Bérczi *et al.* 1988; Juhász 1991).

In the Hungarian literature, the Late Miocene and Pliocene epochs of the Pannonian Basin are commonly referred to as the Lower Pannonian (11.5–5.5 Ma) and Upper Pannonian (5.5–1.2 Ma), respectively. At the beginning of the Lower Pannonian, marine transgression inundated the deepest regions of the high-relief surface, with the elevated islands coming under water later, resulting in strong lateral facies variations. Coastal sandy conglomerates and coarse-grained sandstones, deposited around the islands, may change laterally into siltstones, calcareous marl, limestones and turbidites within distances of a few kilometres, as in the Tótkomlós, Nagykörű and Szolnok Formations, listed in

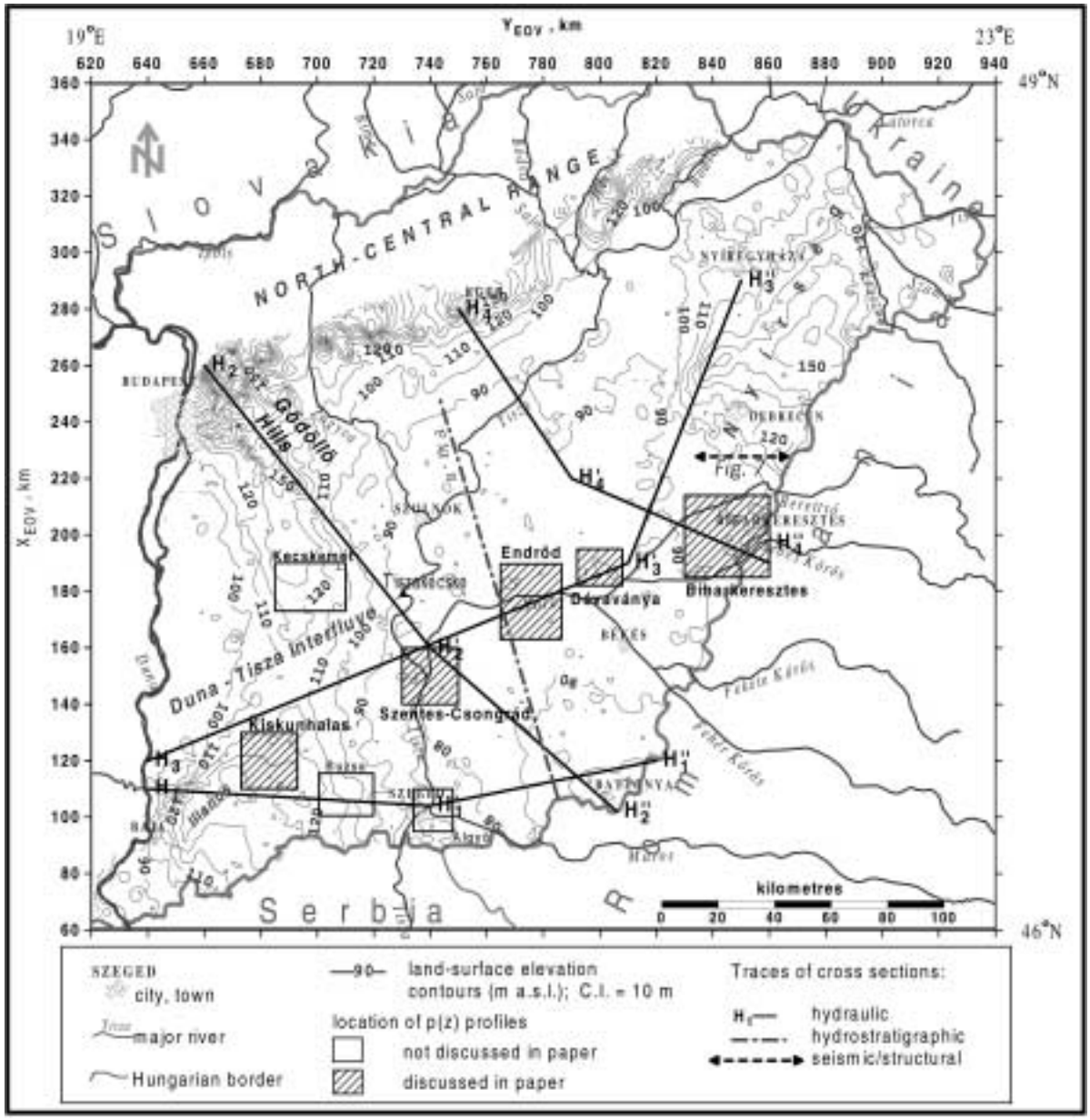

Fig. 2. Topographic map of the study area showing the areas of pressure–elevation profiles, and the traces of: seismic section Ka-27, Fig. 7; hydraulic sections H_1, H_2, H_3, H_4; and hydrostratigraphic section, Fig. 8.

ascending order in Fig. 3, and following the nomenclature introduced by Gajdos *et al.* (1983). The transition from the Lower Pannonian to the Upper Pannonian is marked by regionally widespread deposition of delta slope and near-shore sediments of the Algyő Formation, consisting mainly of mudstones, siltstones and argillaceous marl strata, interbedded with sandstone lenses. The Algyő Formation is, in turn, overlain by the coarsening-upward distributory mouth bar sequence of sandy delta front and delta plain sediments, and the alluvial sandstones, siltstones, clays and marls, some compacted sandstones with calcareous cement and quartz pebble beds, of the Upper Pannonian Törtel and Zagyva Formations. Continued rapid subsidence during the Quaternary (1.2–0 Ma) resulted in the deposition of up to a 1000 m thick sequence of fine- to very coarse-grained, unconsolidated or poorly consolidated clays, claystones, sands, thin-bedded and lenticular gravels of alluvial, fluviatile and eolian origin. The surface geology of the study area is thus characterized by extensive regions of highly permeable loess, sands and gravels.

Tectonic features, such as thrust faults, transform faults and flower structures, have been interpreted to indicate that

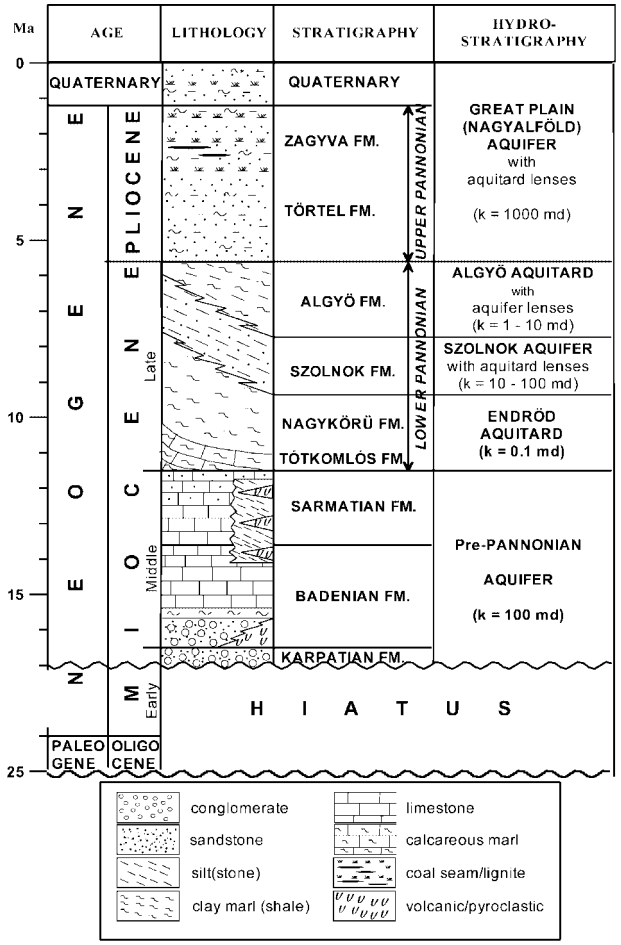

Fig. 3. Lithology, stratigraphy and hydrostratigraphic units in the Great Plain of Hungary.

Fig. 4. Intraplate stresses in the Adria-Alpine-Carpathian-Dinarides region, inferred from structural geology and geophysics (Bada *et al.* 1998, Fig. 12, reproduced with permission).

the former stress regime of crustal extension started to change to a compressional regime at the beginning of the Late Miocene (10.0 Ma). The compressional regime is thought to have been active to date with varying intensity. Its latest major resurgence has been estimated to have started in the Late Pliocene, ≈ 2.5 Ma (Csontos 1995; Gerner *et al.* 1997; Horváth & Cloetingh 1996; Peresson & Decker 1997). Based on an extensive compilation and interpretation of earlier studies and structural geological and geophysical data, Bada *et al.* (1998; Fig. 12) have envisaged the current lateral crustal stresses in regions around the Pannonian Basin as shown in Fig. 4. According to this interpretation, the Pannonian Basin in general, and the Great Plain of Hungary in particular, are at present subject to a compressive stress regime of focally converging sections of the surrounding crustal segments. This interpretation is confirmed quantitatively by satellite geodetic measurements of horizontal velocities of intraplate crustal movements at various stations in the north and north–west parts of the study area proper and to the north and west in the entire Adria–Alpine–Carpathian region (Fig. 5; Grenerczy *et al.* 2000, Fig. 5; Grenerczy *et al.* 2001, Fig. 7; Gy. Grenerczy, personal communication).

A dense network of faults and fractures, created or rejuvenated by intensive Neogene tectonics, has destroyed the regional lithologic integrity of the basement and the basin fill, both in lateral and vertical directions. Depending on the site-specific geological history following tectonic events of faulting and fracturing, the lithologic discontinuities may become highly conductive avenues (Clayton *et al.* 1990) or low–permeability barriers to pore pressure propagation and fluid flow. The regional characteristics of the patterns of Neogene age faults can be seen in Fig. 6, as adapted from Rumpler & Horváth (1988; Fig. 11). The dominant orientation of the faults is NE–SW, but several faults strike also NNE–SSW or even WNW–ESE. There are numerous deep sedimentary troughs in the area, usually bounded by normal faults. Many of these normal faults, and thus their associated grabens, are dissected by strike-slip faults, possibly effecting significant lateral displacements of the disconnected and juxtaposed graben sections. Curving, splaying and side-stepping of strike-slip fault segments are common.

A characteristic and important structural style is shown in Fig. 7, adapted from Rumpler & Horváth (1988; Fig. 9). The location of the seismic section is shown in Figs 2 and 6. The section Ka–27 (Fig. 7; Rumpler & Horváth 1988, Fig. 9) shows normal faults, some penetrating the basement, their listric nature and lateral spacing, flower structures, folding and vertical displacements of strata. Many of the major faults dissect the entire thickness of the rock framework from the basement to the Upper Pannonian, and some even reach into the Quaternary. Owing to the density, geometry and frequent splaying of the faults, different bore holes located just short distances apart can penetrate different faults at similar elevations and with connections to different strata. This

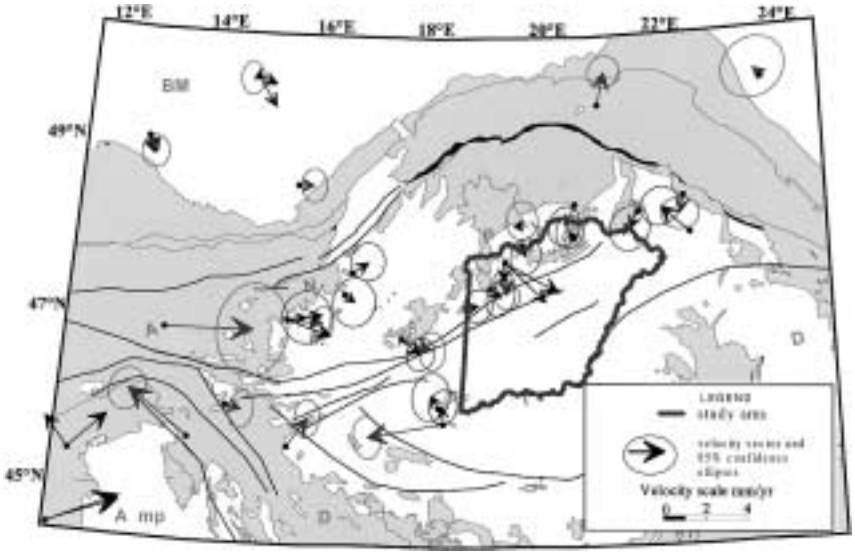

Fig. 5. Intraplate crustal velocities in the Adria–Alpine–Carpathian-Dinarides region, based on Global Positioning System satellite geodetic surveys (modified from Grenerczy *et al.* 2001; courtesy of Gy. Grenerczy, personal communication, and with the permission of the European Geophysical Society).

observation will be used in the interpretation of vertical pore pressure profiles in later sections.

HYDROSTRATIGRAPHY

Hydrostratigraphic classification was developed from original petroleum industry records of measured core permeabilities and DST reports, and from information found in in-house reports and published papers. Whereas it was difficult to distill regionally representative permeability values from the wealth of information organized and processed for other purposes, one feature stands out clearly: matrix permeabilities are generally high in the entire basin, including those of the marl– and shale–dominated aquitards. The following examples of independent permeability estimates serve to illustrate the point.

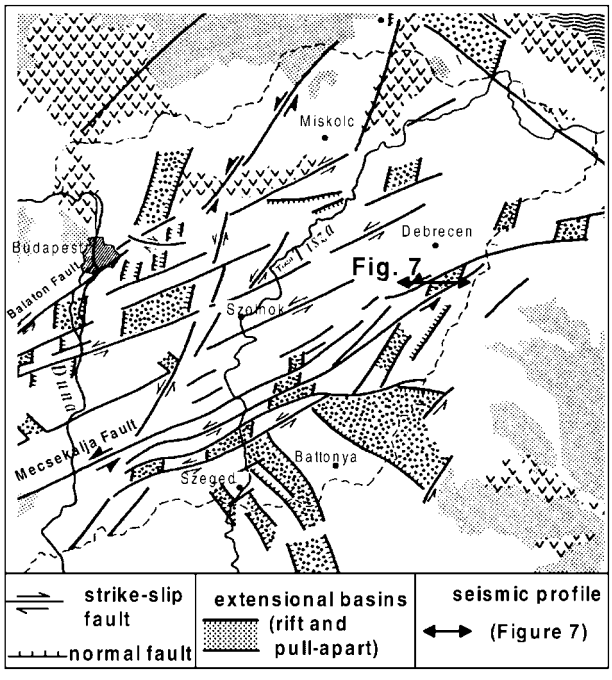

Fig. 6. Regional patterns of Neogene age faults in the Great Plain of Hungary, and trace of seismic section Ka-27, Fig. 7 (modified from Rumpler & Horváth 1988, fig. 11).

Palaeozoic metamorphics and Lower and Middle Triassic carbonates of the basement: 1–10 md (Bérczi & Kókai 1976). Pliocene–Pleistocene: aquitards, 10–10^2 md; aquifers, 10^3–10^5 md (Halász 1975). Lower Pannonian: lower, (3–5) $\times$ 10 md; middle, 5 $\times$ 10–4 $\times$ 10^3 md; upper, (2–5) $\times$ 10^2 md. Upper Pannonian: lower and middle, 5 $\times$ 10^2–10^3 md; upper, > 10^3 md (Korim 1966). Pliocene aquifer system, 5×10^2–5×10^3 md; Quaternary aquifer system, 10^3–10^4 md (Alföldi *et al.* 1978). At depths of: 1600–1800 m, 4 $\times$ 10^2 md; 1800–2000 m, 2.7 $\times$ 10^2 md; below 2000 m, 2.2 $\times$ 10^2 md (Korim & Liebe 1973). Mesozoic, 10^{-1} md; Mesozoic–Miocene, 10^{-1}–7.5 $\times$ 10 md; Eocene–Oligocene, 10^{-1}–10^2 md; Miocene, 8.5 $\times$ 10–2.3 $\times$ 10^2 md; Sarmatian (2–6) $\times$ 10–10^2 md; marls <10^{-1} md; Lower Pannonian, 10^{-1}–4 $\times$ 10^2 md (Pap 1976). Aquitards, 10^{-2}–10 md; aquifers, 10^3–10^5 md (Szebényi 1955). Only two documents were found that gave quantitative data on anisotropy of the matrix permeability. Korim (1966; p. 527) reports that the vertical permeability is '30-50%' less than the horizontal one in Pannonian sands and sandstones. In an anonymous and undated in-house oil company report, analysing 'thousands of core permeability measurements', marls show a permeability anisotropy of slightly greater than one order of magnitude in the depth range of $\approx$ 1–2 km. Their permeability is shown to be uniformly less than 10^{-1} md below $\approx$ 2.5 km. The degree of anisotropy reported for sandstones does not exceed one–half of an order of magnitude anywhere between 1 and 5 km depth. Sandstone permeability is

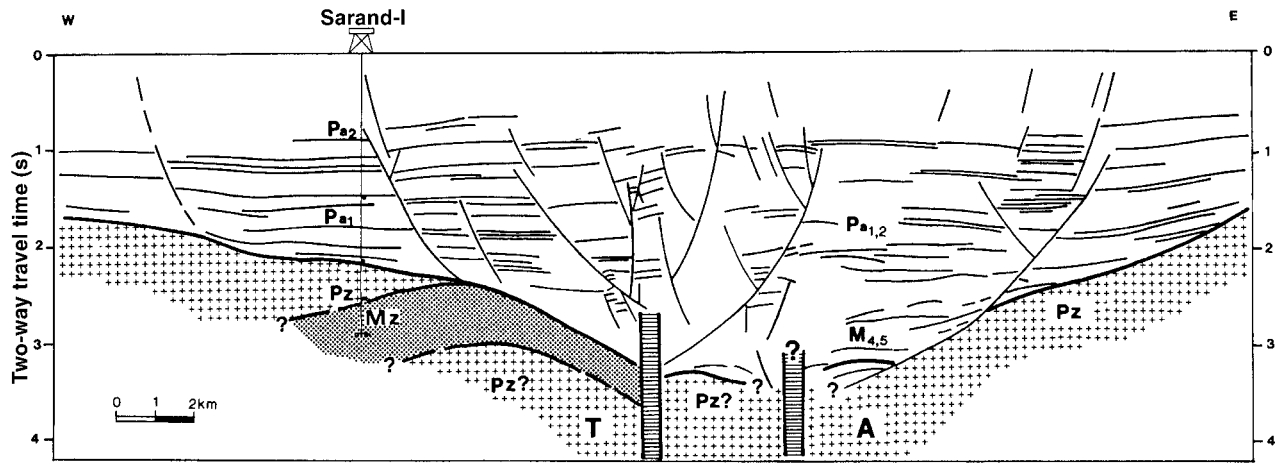

Fig. 7. Line drawing interpretation of seismic section Ka-27, illustrating a structural style in the Great Plain of Hungary (Rumpler & Horváth 1988, fig. 9, reproduced with the permission of the American Association of Petroleum Geologists).

shown to decrease to the range of (1–2) $\times$ 10^{-1} md at a depth of $\approx$ 5 km.

Based on considerations of chronostratigraphic divisions, lithologic facies types and reported values of permeabilities as exemplified above, the subsurface has been subdivided into six regional hydrostratigraphic units, as follows (Figs 2, 3 and 8).

(1) *Pre-Neogene Aquiclude:* the lowermost hydrostratigraphic unit. It is considered to form the basal boundary of negligible permeability of the flow domain. Its top surface runs within the body of the Pre-Pannonian rocks, but its depth and exact shape cannot be established from available data. Inferred from general considerations concerning the effects of subaerial erosion and tectonic events on the development of permeability patterns in mountainous regions, it is assumed that the near-zero permeability surface of the Pre-Neogene Aquiclude is a reduced amplitude replica of the topography of the Pre-Pannonian rocks.

(2) *Pre-Pannonian Aquifer:* a major aquifer at the base of the flow domain, made up of the Middle Miocene Badenian

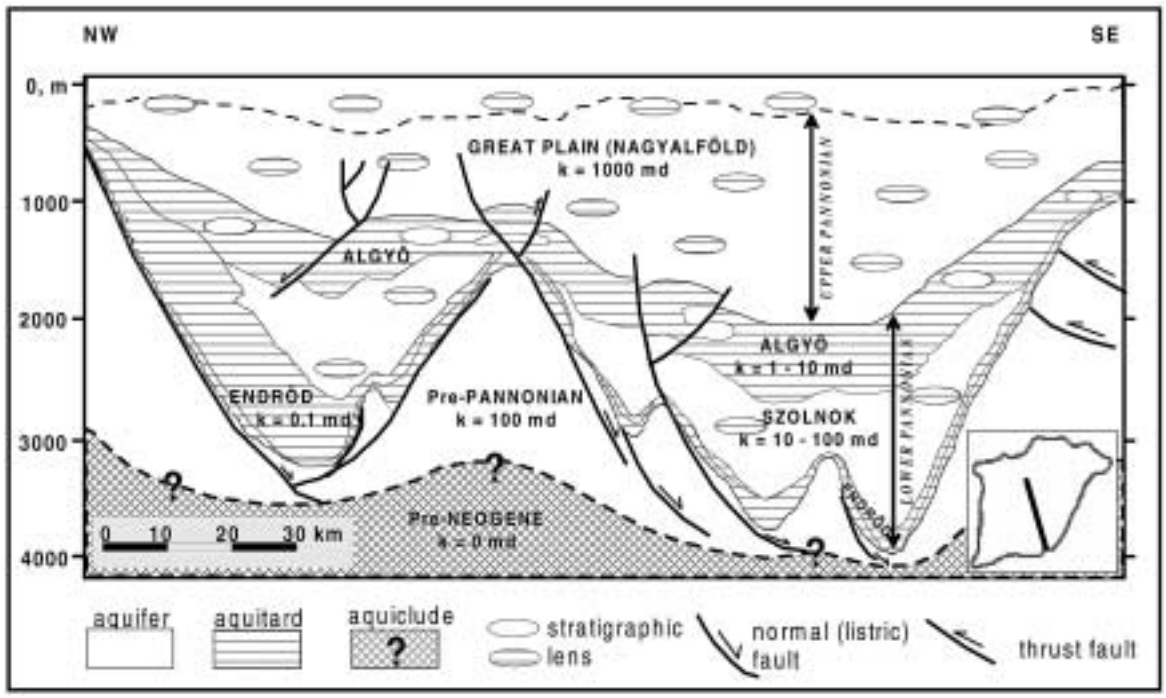

Fig. 8. Schematic NW-SE hydrostratigraphic section across the Great Plain of Hungary (based on Juhász 1991, fig. 7, with the permission of the American Association of Petroleum Geologists).

and Sarmatian Formations. Its high permeability is due to tectonic fracturing and faulting, the abundance of coarse-grained arkosic rocks and the remnant effects of subaerial weathering. The hydraulic interpretation of the lithologic properties is corroborated by DST and core analyses, conducted in the course of intensive exploration for petroleum. The aquifer contains numerous high-yielding oil and gas reservoirs.

(3) *Endrőd Aquitard:* a regionally extensive but discontinuous unit primarily of low-permeability calcareous and argillaceous marls. At several places where it is absent, the subjacent (Pre-Pannonian) and overlying (Szolnok) aquifers are in contact, thus in direct cross-formational hydraulic communication.

(4) *Szolnok Aquifer:* a cyclic alternation of consolidated sandstones, siltstones and clay–marl beds of a prodelta turbidite facies. It is regionally discontinuous and occurs only in the deep subbasins, above deep basin marls. Where it pinches out against the flanks of the basement highs, the Endrőd Aquitard is overlain directly by the next higher unit, the Algyő Aquitard.

(5) *Algyő Aquitard:* an areally extensive unit of poorly to well-consolidated siltstone and clay–marl, containing relatively highly permeable sand lenses of reworked turbidites, rhythmic mouth bar sequences or submarine channel fills. Above basement highs, the lithology is sand-dominated, giving aquifer properties to the regional aquitard locally. Owing to its lenticularity and other sedimentological discontinuities, as well as to cross-cutting by faults and fractures, the Algyő Aquitard is leaky in nature.

(6) *Great Plain (Nagyalföld) Aquifer:* a major unit, dominated by unconsolidated coarse clastics (sand, gravel, loess), and containing relatively thin clay and silt beds of varying lateral extent. It includes the Upper Pannonian Törtel and Zagyva Formations, and the surficial Quaternary sediments which cover the entire basin to a thickness of 2400 m. Its chief lithologic characteristic is a predominance and good spatial connectivity of the highly permeable bodies of silts, and coarse sands and gravels. Large amounts of groundwater are pumped at high rates from the upper part of this aquifer, while thermal water is extracted from its basal Törtel Formation for health spas and heating.

On the basis of lithologic, stratigraphic and structural considerations, the entire porous and permeable framework of the study area can be considered as a regional and cross–formational hydraulic continuum, with the base at depths below the top of the Pre-Pannonian aquifer and with the land surface being the upper boundary. Our goal is to use this understanding of the geological framework as a guide for the interpretation of the mapped fluid potential patterns. The hydraulic properties of the various units can only be represented in a generalized, order–of–magnitude sense: permeability contrasts are indicated in Fig. 3.

The climate of the Pannonian Basin is temperate–continental with mild winters (minimum, − 20°C) and hot summers (maximum, up to 40°C). The significant aspect of the climate in the present context is the fact that groundwater recharge is sufficient to maintain the water table near the land surface, generally within 2–5 m in the highlands and 0–2 m in the lowlands. Consequently, the configuration of the water table remains a close replica of the topographic relief at all times, and it can thus be considered as the upper boundary of the basin's flow domain.

BASINAL FLUID POTENTIAL: PATTERNS AND INTERPRETATION

In basin–scale characterization of subsurface flow fields, the most critical term to evaluate correctly is the hydraulic head, h. Its perceived regional pattern serves as the basis for the interpretation of the distribution of the fluid potential and its gradient, the fluid driving force (Hubbert 1940, 1953). Flow is always in the direction of decreasing hydraulic head because h is directly proportional to the fluid's potential energy Φ:

$$h = \Phi/g \tag{1}$$

where Φ is the mechanical energy per unit mass of fluid. If we assume constant fluid density along the flow path and neglect inertial forces, then

$$\Phi = gz + p/\rho \tag{2a}$$

and

$$h = z + p/\rho g \tag{2b}$$

where z is the elevation of the measurement point with respect to a datum plane, usually sea level, and p is pore pressure; thus, all components of h are measurable.

In equation 2b, $\rho g = \gamma$ is the specific weight of the fluid, which is numerically equal to the vertical pressure gradient in a column of static fluid of density ρ. The variables used in the present study were the hydraulic head, h, pore fluid pressure, p, and the vertical pressure gradient, γ. These parameters were derived from measured values of well water levels and pore pressures. In calculating h from pore pressures, the pore water density was assumed to be uniformly 1000 kg m^{-3}, as the total dissolved solids content of the vast majority of water samples is less than 2 g L^{-1}, and the maximum values remain below 30 g L^{-1}. Accordingly, the value assumed for the vertical hydrostatic, or 'nominal', pressure gradient is γ_{st} = 9.8067 MPa km^{-1}.

Pressure–elevation profiles, $p(z)$

The pressure–elevation profile, $p(z)$, is a plot of the pore fluid pressures versus the topographic elevation of the measurement points along a vertical beneath a given location in the field (Figs 9–13). In such a plot, the pressure difference over a unit vertical distance is numerically equal to the vertical

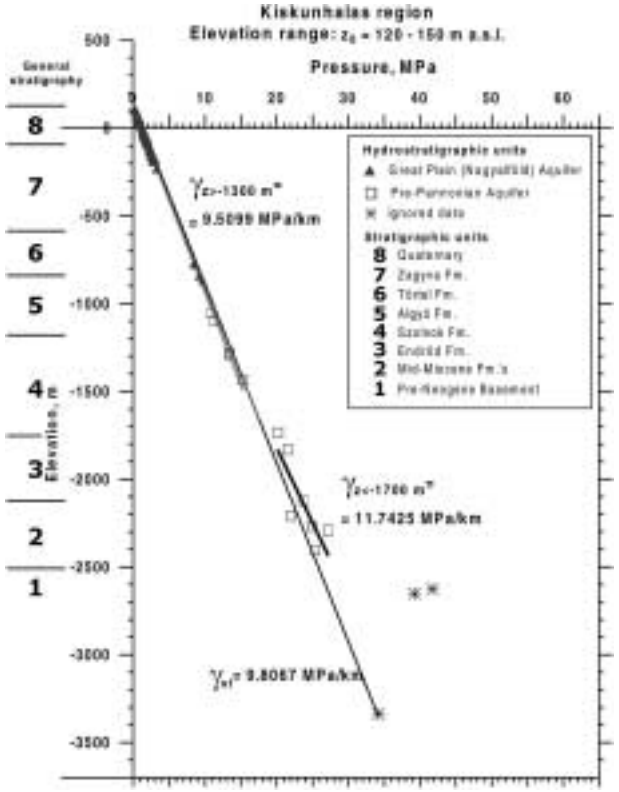

Fig. 9. Pressure-elevation profile, $p(z)$, Kiskunhalas region (for location, see Fig. 2).

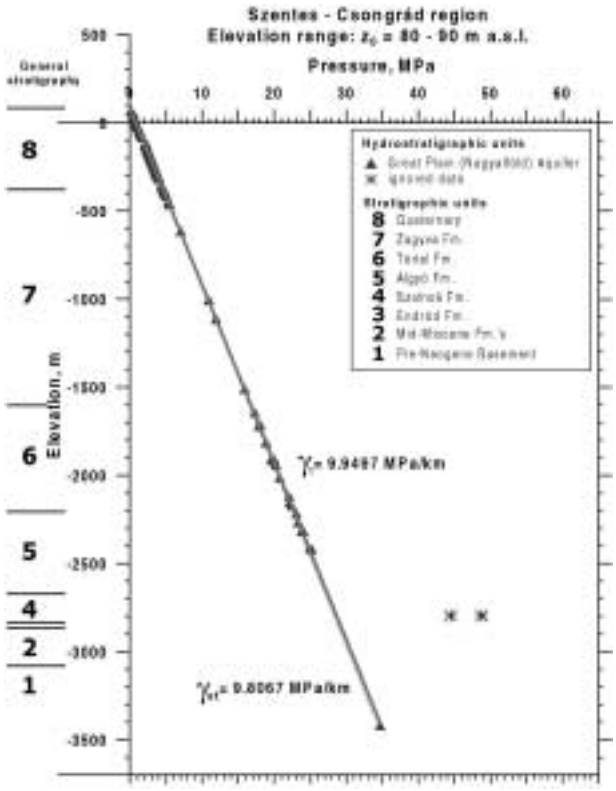

Fig. 10. Pressure-elevation profile, $p(z)$, Szentes-Csongrád region (for location, see Fig. 2).

component, γ, of the pressure gradient at the specified elevation and is therefore indicative of the vertical sense of the fluid impelling force. In the case of fresh water (ρ = 1000 kg m^{-3}), a hydrostatic value of γ_{st} = 9.8067 MPa km^{-1} indicates stagnation of water or horizontal flow. Values that are less or greater than γ_{st}, i.e. $\gamma_{dyn} < \gamma_{st}$ or $\gamma_{dyn} > \gamma_{st}$, indicate a force component driving the water downwards or upwards, respectively. A sharp break in the pressure profile reflects an abrupt change in the pressures or pressure gradient beneath the given site. Generally, such changes result from significant vertical changes in the permeability of the rock framework. Conversely, a pressure profile or its segments that are devoid of breaks in direction imply relatively homogeneous rocks over the depth intervals of the straight portions.

Eight pressure–elevation profiles were constructed for the present purpose (Fig. 2), five of which are discussed here to exemplify the different styles of the one-dimensional vertical pressure distribution in the study area. Ideally, a $p(z)$ profile should be constructed from continuous and simultaneous measurements taken under one surface point along one single vertical in a homogeneous fluid environment. In real life, such ideal situations do not exist and the requirements must be relaxed. Accordingly, data from several wells were combined into single $p(z)$ profiles so as to increase control point density. In order, however, to reduce the effects of rock heterogeneities and topographic elevation differences, both the size and relief of the areas from which the wells were used for individual $p(z)$ plots were kept to a minimum.

Kiskunhalas (area boundaries: X_{EOV} = 110–130 km (20 km), Y_{EOV} = 673–693 km (20 km); land surface elevation: 120 m < z_0 < 150 m a.s.l.; elevation of pressure measurement domain: $z = z_0 > -3350$ m)

The area is located on the central highland of the Duna–Tisza interfluve and includes the highest elevation range of its southern regions. The $p(z)$ profile consists of two straight segments which have distinctly different gradients and intersect at the elevation of $z \approx -1300$ m (Fig. 9). The gradient in the top segment is substantially less than hydrostatic, $\gamma_{z>-1300}$ = 9.5099 MPa km^{-1} < γ_{st} = 9.8067 MPa km^{-1}, while that of the one below $z = -1700$ m is superhydrostatic, $\gamma_{z<-1700}$ = 11.7425 MPa km^{-1} > γ_{st} = 9.8067 MPa km^{-1}, indicating downward and upward driving forces, respectively.

Descending flow beneath the highest regions of the Duna–Tisza interfluve can be explained by gravity drive. The superhydrostatic gradient of the lower segment requires an energy source below $z = -2500$ m. The existence of such an energy source is qualitatively supported by the two points of still higher pressure ($\approx$ 40 MPa) at $z \approx -2650$ m in the

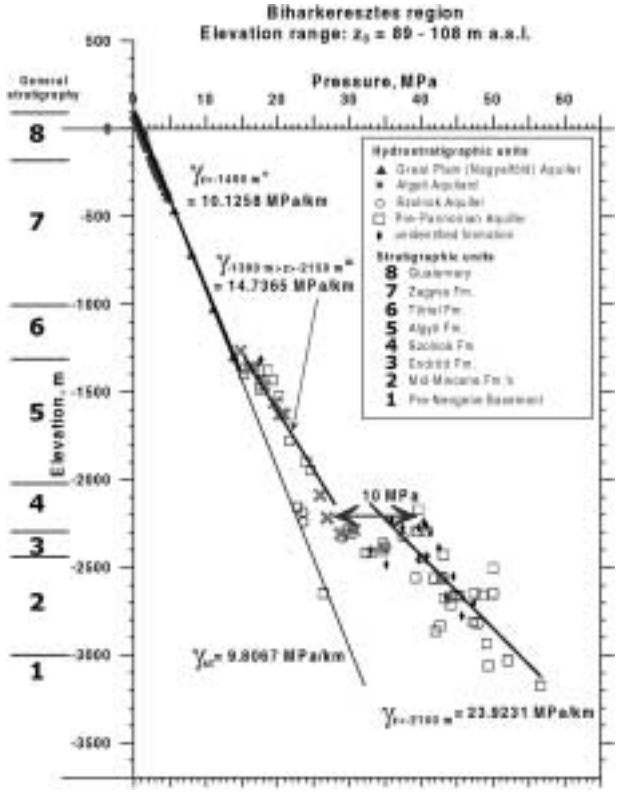

Fig. 11. Pressure-elevation profile, $p(z)$, Biharkeresztes region (for location, see Fig. 2).

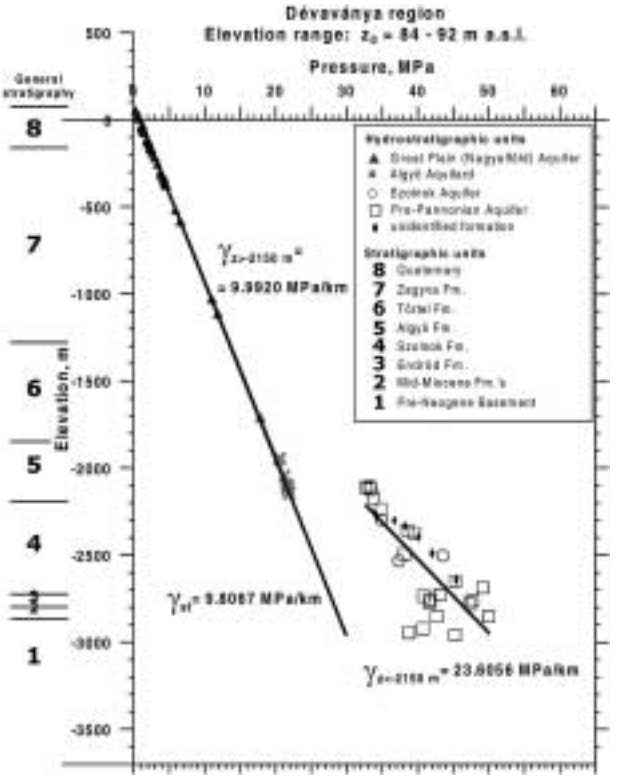

Fig. 13. Pressure-elevation profile, $p(z)$, Dévaványa region (for location, see Fig. 2).

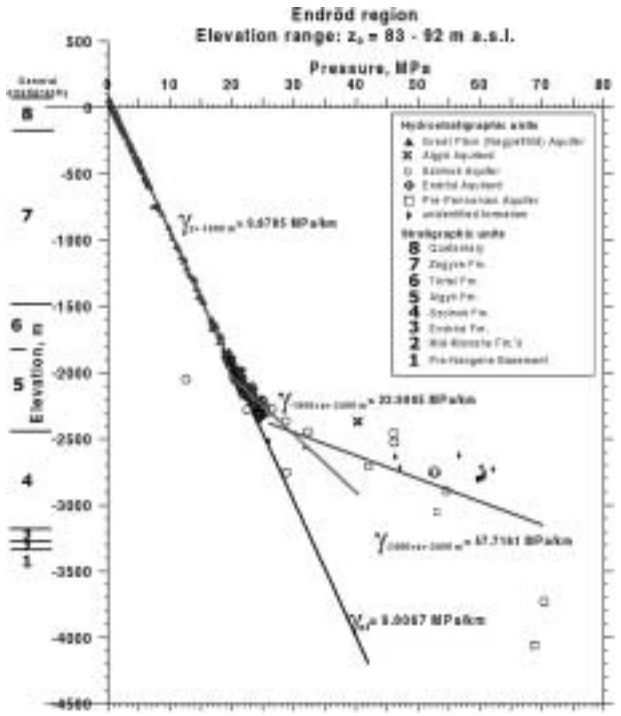

Fig. 12. Pressure-elevation profile, $p(z)$, Endrõd region (for location, see Fig. 2).

Pre-Neogene basement. However, two points are considered insufficient to warrant the assignment of a gradient value.

A high degree of vertical hydraulic communication across various lithologic units can be inferred from the straightness of the two segments of the profile. This feature has a particular significance in the approximate elevation range of $-850\ \text{m} > z > -1150$ m, indicating ready cross-formational flow through the ≈ 300 m thick Algyõ Aquitard.

Szentes–Csongrád (area boundaries: X_{EOV} = 140–160 km (20 km), Y_{EOV} = 730–750 km (20 km); land surface elevation: 80 m < z_0 < 90 m a.s.l.; elevation of pressure measurement domain: $z = z_0 > -2900$ m)

The sample block is located along the Tisza River in one of the lowest regions of the study area. The $p(z)$ profile is a straight line with dense data control down to an elevation of $z \approx -2400$ m (Fig. 10). The vertical pressure gradient is slightly superhydrostatic, $\gamma_{z > -2400}$ = 9.9497 MPa km^{-1}, indicating an upward driving force across the entire depth range. Owing to the low topographic position of the area, the assumption of gravitational discharge, at least in the upper strata, is warranted. The definition of a boundary between flow driven upward by gravity and that driven by a deep internal energy source, however, is not possible. Two measurements at $z \approx -2800$ m show a high average overpressure of $p \approx 47$ MPa. Similar to the Kiskunhalas case, it

is difficult to assign a pressure gradient value based only on two points. However, the existence of such high pressures is corroborated by similar values at those depths in the area (e.g. at ≈ 120 km in Section H_2, Fig. 21) and point to other driving forces in or below the Pannonian Aquifer.

Good hydraulic communication between the Algyő Aquitard and the overlying Great Plain (Nagyalföld) Aquifer (Fig. 3) can be inferred from the straightness of the profile at the level of the boundary between these two hydrostratigraphic units, i.e. at $z \approx -2200$ m (Fig. 10). On the other hand, a high hydraulic resistance at the lower boundary of the Algyő Aquitard, at $z \approx -2675$ m, against flow forced upwards across the Szolnok Aquifer by the postulated deep energy source may explain the strong overpressures below.

Biharkeresztes (area boundaries: X_{EOV} = 185–214 km (29 km), Y_{EOV} = 830–860 km (30 km); land surface elevation: 89 m < z_0 < 108 m a.s.l.; elevation of pressure measurement domain: $z = z_0 > -3175$ m)

Three well-defined and one questionable segment can be distinguished on the Biharkeresztes $p(z)$ profile (Fig. 11). The top segment, above $z > -1400$ m, with $\gamma_{z > -1400} = 10.1258$ MPa km^{-1} is suggestive of upward-directed, gravity-driven flow, possibly enhanced by high pressures dissipating from the segment below. The gradient of the lowest segment, below $z \approx -2150$ m, is significantly greater than hydrostatic, $\gamma_{z < -2150} = 23.9231$ MPa km^{-1}, and is consistent with a source of high pressure below the deepest point of measurement at $z \approx -3175$ m. The transitional middle segment, between $z \approx -1300$ and -2150 m (a thickness of ≈ 850 m), appears to reflect a gradual loss of pressure energy of water ascending cross-formationally over more than 800 m of the low-permeability Algyő Aquitard, impelled by the high overpressures below. The four pressure values along the normal hydrostatic gradient line at depths of $z \approx -2100$ to -2600 m are attributed to production effects and are not considered to be representative of natural conditions.

A noteworthy feature of the pressure profile is a wide band of observed pressures in the bottom segment; its width may exceed 10 MPa at some given elevation levels. This feature can be explained by assuming that pressures were measured in points at approximately the same elevations, but in wells at different locations that have penetrated several faults or sedimentary discontinuities of different permeabilities, and of different degrees of hydraulic communication with a deep-seated source of high pressure. From another viewpoint, the close similarity of pressure values over the depth range of 400–600 m can also be understood by assuming that several of the above-mentioned, possibly low-angle, faults are situated above one another (as, for example, shown in Fig. 7) and penetrated by a few closely spaced bore holes. The probability of faulting, tectonic displacement and stratigraphic and lithologic discontinuities is apparent from the frequent co-occurence of several hydrostratigraphic units of significantly different age at similar elevation levels. Attention is drawn also to the large number of pressure measurements conducted in the Algyő Aquitard over the depth range of $z \approx -1250$ to -2300 m. The obvious interest of petroleum explorationists in this 'aquitard' clearly demonstrates its potential to contain producible reservoirs, i.e. highly permeable rock bodies. The hydraulically conductive nature of the Algyő Aquitard, at least in the Biharkeresztes block, is also corroborated by the relative straightness of the middle segment of the $p(z)$ profile.

Endrőd (area boundaries: X_{EOV} = 163–190 km (27 km), Y_{EOV} = 764–787 km (23 km); land surface elevation: 83 m < z_0 < 92 m a.s.l.; elevation of pressure measurement domain: $z = z_0 > -4050$ m)

The Endrőd block is located in the central and lowest regions of the Great Plain. The basic configuration of its $p(z)$ profile resembles that of Biharkeresztes: three straight–line segments with monotonically increasing gradients downwards (Fig. 12). The top segment's gradient is slightly superhydrostatic, $\gamma_{z > -2100} = 9.8785$ MPa km^{-1}, indicating uniformly ascending flow through a regionally homogeneous rock body above the elevation level of $z \approx -2100$ m. The bottom segment, between approximately -2400 and -3100 m elevations, is strongly overpressured with an apparent vertical pressure gradient of $\gamma_{-2400 > z > -3100} = 57.7161$ MPa km^{-1}, which is more than twice lithostatic! The middle segment's gradient is determined at $\gamma_{-2100 > z > -2400} = 22.9995$ MPa km^{-1}, taken over a vertical distance of ≈ 300 m (between -2100 and -2400 m), i.e. barely more than one-third of the 850 m thickness of the Biharkeresztes middle segment.

The force and therefore the flow conditions indicated by the top segment are consistent with those expected in an ascending flow domain due either to gravitational discharge and/or a deep-seated energy source. However, if water in this domain is derived, indeed, from two different origins, i.e. meteoric driven by gravity and 'depth water' driven by a deep pressure source, the region and depth zone where they merge, or the boundary between them, cannot be determined from an analysis of the $p(z)$ profile; the boundary, if there is one, could be at any level above $z = -2100$ m.

The simple linear interpretation of the bottom segment's pressure distribution, as shown in Fig. 12, is considered to be illusory. Instead, a more realistic interpretation would probably be a series of separate, and perhaps subparallel, gradient lines of slightly greater values than that at the middle section, but less than lithostatic, i.e. less than ≈ 25.5 MPa km^{-1}. This interpretation invokes the same conceptual image as used to explain the wide band of overpressures in the bottom segment of the Biharkeresztes profile. However, multiple gradient lines cannot actually be proposed because of a lack of adequate constraints on their possible position and orientation.

A fundamental difference between the Biharkeresztes and Endrőd profiles seems to be the significantly lower elevation, i.e. greater depth, of the top of the overpressured zone at Endrőd ($z \approx -2100$ m) than at Biharkeresztes ($z \approx -1400$ m). On the other hand, at the elevation level of $z \approx -3000$ m pressures are in the range of 55–60 MPa in both cases. It is suggested, therefore, that the unrealistically high gradient of the bottom segment of the Endrőd profile is, indeed, only 'apparent', and that it is due to a combination of the presence of a relatively thin (≈ 300 m) but low-permeability aquitard situated at a depth below $z = -2100$ m, effectively confining a number of distinct lithologic discontinuities of different hydraulic conductivities, which are connected to a deep-seated pressure source. In other words, the low position of an effective local seal, combined with high overpressures at a given depth, results in reduced thickness of the zone of transition from overpressures to normal pressures.

Dévaványa (area boundaries: X_{EOV} = 182–195 km (13 km), Y_{EOV} = 792–808 km (16 km); land surface elevation: 84 m < z_0 < 92 m a.s.l.; elevation of pressure measurement domain: $z = z_0 > -3000$ m)

The Dévaványa $p(z)$ profile consists of two segments only (Fig. 13). The top one is a well-constrained straight line reaching to the bottom of the Algyő Aquitard at $z \approx -2150$ m, at a slightly superhydrostatic gradient of $\gamma_{z>-2150} = 9.9920$ MPa km^{-1}. It is interpreted to indicate conditions seen in the upper segments of the other $p(z)$ profiles (Szentes–Csongrád, Biharkeresztes, Endrőd), i.e. uniformly ascending meteoric water driven by gravity with a possible contribution of 'depth water' driven by a deep pressure source.

The bottom section, again, is less well constrained than the top one, but better than those in the previous cases. The lower scatter of the data points is probably due to the lower number of formations tested and the smaller block size.

The significant feature in this example is the absence of a transitional segment between the overpressured and normally pressured zones. The phenomenon can be explained by the presence of a local seal effectively capping the few avenues available for fluid flow and pressure dissipation. That some diffusion is still taking place is indicated by the strong superhydrostatic gradient. If the seal at the top were ideally effective, the pressures would abruptly increase directly beneath it until the gradient reached hydrostatic value over the entire depth range, while the pressures at the bottom remained unchanged. The pressures at the bottom keep reflecting the strength of their source at depth or, at least, the part of that strength reaching up to their points of measurement.

Summary

In summary, the following observations and inferences have been made from all eight pressure profiles analysed in the study, including the three reported elsewhere (Tóth & Almási 1998).

(1) Two vertically superposed principal pore pressure zones can be recognized in the area: an unconfined upper one, and a confined and overpressured lower one; a transitional zone may connect the two zones in places.

(2) Superhydrostatic vertical pressure gradients increase monotonically with depth below the upper boundary of the zone of overpressures.

(3) The depth to the upper boundary of the zone of overpressures is not controlled by hydrostratigraphy or depth, e.g.

Kiskunhalas: at −1600 m Szolnok Aquifer, base (Fig. 9).

Biharkeresztes: at −1300 m Algyő Aquitard, top (Fig. 11).

Dévaványa: at −2100 m Algyő Aquitard, base (Fig. 13).

(4) Water flow is driven by gravity in the upper, unconfined zone, and by a high-pressure energy source seated below the top of the Pre-Pannonian Aquifer in the lower, confined zone.

(5) The regionally unconfined nature of the flow in the upper zone is indicated by the consistently and strictly straight-line character of the $p(z)$ profiles above the top of overpressures.

(6) Gravity drive is indicated by: (i) vertical pressure gradients less than hydrostatic, $\gamma_{actual} < \gamma_{static}$, beneath topographically high regions: a characteristic condition of descending groundwater flow, i.e. recharge (e.g. Kiskunhalas, Fig. 9); (ii) pressure gradients greater than hydrostatic, $\gamma_{actual} > \gamma_{static}$, beneath topographically low regions: characteristic of ascending groundwater flow, i.e. discharge (e.g. Biharkeresztes, Fig. 11; Dévaványa, Fig. 13).

(7) A deep-seated energy source is indicated by the existence and ubiquity of superhydrostatic vertical pressure gradients below the top of the Pre-Pannonian Aquifer. This type of pressure field induces uniformly upward orientated flow in the domain.

(8) The broad band of overpressures at given elevation levels is due to the presence of multiple pathways (fracture zones, faults, sediment windows) of differing hydraulic resistance to fluids being driven upward.

Tomographic fluid potential maps, $h_{ij}(x,y)$

A tomographic fluid potential map, $h_{ij}(x,y)$, is a contoured projection of hydraulic head values in the x–y plane determined in a horizontal subsurface domain of constant thickness and specified elevation. In a map, h is the hydraulic head in, and x and y are the horizontal EOV coordinates of, the point of measurement; i and j are, respectively, the elevations of the upper and lower boundaries of the domain of measurement. Elevation z of the measurement point is always $i \geq z \geq j$. A full portrayal of the potential distribution in a given rock volume generally requires several tomographic maps.

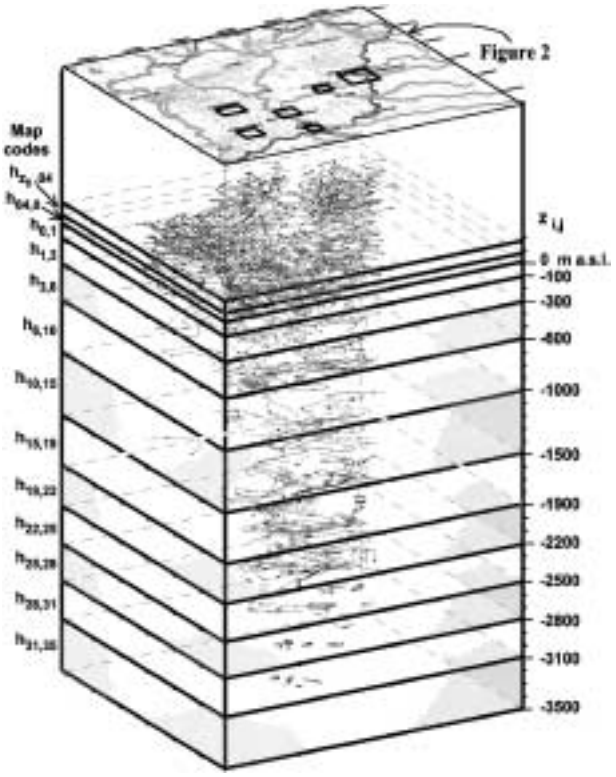

Fig. 14. Column of tomographic fluid potential maps, $h_{ij}(x,y)$, showing map codes and elevation intervals of the mapped rock slices.

The rock framework of the study area was first divided into 13 horizontal slices. The position and thickness of the slices were defined, so as to ensure maximum data point concentration within the boundaries of individual slices, as well as to minimize the number and magnitude of vertical pressure changes within the slices. Details of the nomenclature, positions, dimensions and data point control of the rock slices are given in Fig. 14 and Table 1. Only five examples of the 13 fluid potential maps prepared for the study are presented here. Characteristics of the potential field identified on these maps are consistent with those seen on the other eight maps. The full set of maps is included in an unpublished report (Tóth & Almási 1998).

Tomographic fluid potential maps $h_{z0,04}$ and $h_{1,3}$

The potential maps $h_{z0,04}$ and $h_{1,3}$ (Figs 15 and 16) show the hydraulic head distribution in the 40 m thick uppermost rock framework slab and in the slab bounded by the horizontal planes at $z = -100$ m and $z = -300$ m elevations, respectively (Table 1).

Three major regional properties characterize the fluid potential distribution in the elevation range between the land surface and $z = -300$ m: (i) the fluid potential surfaces resemble the configuration of the land surface; (ii) hydraulic head values decline with increasing depth in regions of high topography; and (iii) hydraulic heads increase with depth

Table 1 Map codes and principal data of the tomographic rock framework slices.

Map code ($h_{i,j}$)	Top z_i (m)	Thickness $d_{i,j}$ (m)	Data points (n)
$h_{z0,4}$	Land surface, z_0	≈ 40	2304
$h_{4,0}$	$z_0 - 40$	75–140	5120
$h_{0,1}$	0	100	3692
$h_{1,3}$	-100	200	2547
$h_{3,6}$	-300	300	891
$h_{6,10}$	-600	400	464
$h_{10,15}$	-1000	500	339
$h_{15,19}$	-1500	400	331
$h_{19,22}$	-1900	300	281
$h_{22,25}$	-2200	300	196
$h_{25,28}$	-2500	300	106
$h_{28,31}$	-2800	300	66
$h_{31,35}$	-3100	400	49

under regional lowlands. This type of potential distribution is known to indicate gravity-driven flow regimes in regionally unconfined flow domains (Freeze & Witherspoon 1967; Tóth 1963, 1995). Principal regions of descending flow, i.e. groundwater recharge, are: the central ridge of the Duna–Tisza interfluve, in general, and its prominently elevated northern and southern parts, in particular, namely the Gödöllő Hills and Illancs (Fig. 2); the North Central Range along the study area's northern border; and the sandy hills of the Nyírség, in the north-east. The fluid potentials do not change perceptibly with depth along the ≈ 100 m hydraulic head contour line, which itself follows closely the 100 m topographic contour on both flanks of the ridge. This belt of transition, or lateral flow, is at a slightly higher elevation of ≈ 100–110 m in the Nyírség. The main regional discharge areas are a 5–25 km wide belt along the east bank of the Duna River, and the coalescing broad plains along the Tisza River and the Körös River system, the latter two together forming the core area of the Great Plain. The rise in head with depth beneath the plains is definite but only a few metres large. The small magnitude is probably due to the significantly larger size (more than double) of the discharge area than that of the recharge areas, and the high permeability.

Tomographic fluid potential maps $h_{3,6}$, $h_{10,15}$ and $h_{22,25}$

The relief of the hydraulic head surface in the rock slab of $i = -300$ m $\geq z \geq -600$ m $= j$ ($h_{3,6}$ map, Fig. 17) continues to show the gradual downward attenuation observed in the shallower sections, but it still retains the relatively high potentials in the regions of the interfluve, North Central Range and the Nyírség (Fig. 2). However, as a new feature, islands of 'potential mounds' appear at a few locations, thus reversing the trend of the hydraulic head's downward decline. For example, in the general area of $X_{EOV} = 80$–140 km, $Y_{EOV} = 660$–700 km, hydraulic heads decline from the near-surface values of $h \approx 130$–140 m to $h \approx 120$ m in the

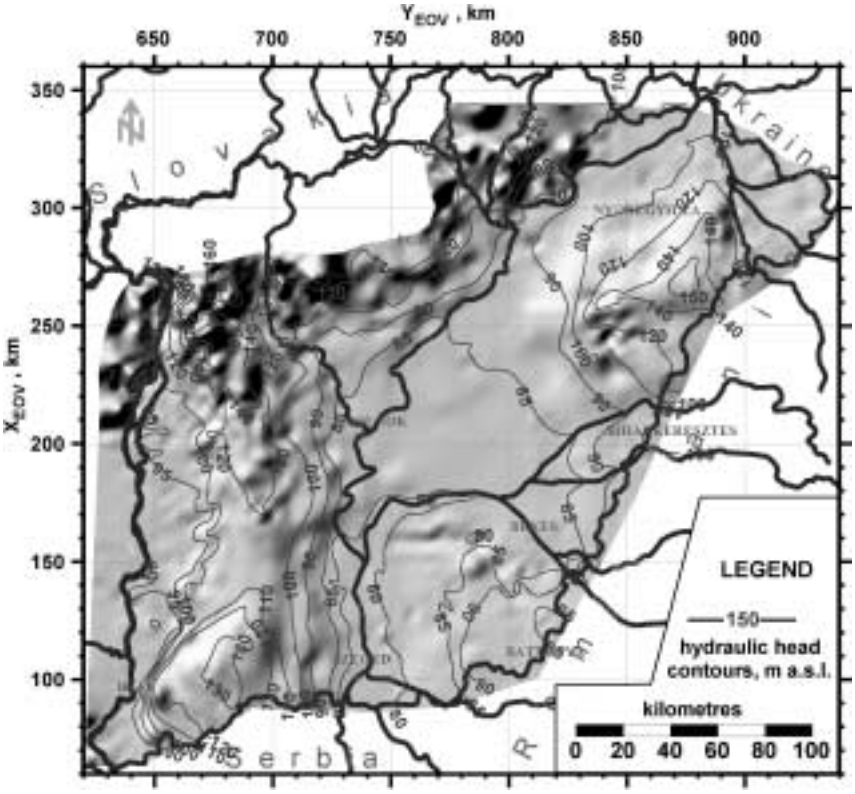

Fig. 15. Tomographic fluid potential map, $h_{z0,40}$, based on 2304 measurement points between the land surface, z_0, and 40 m depth.

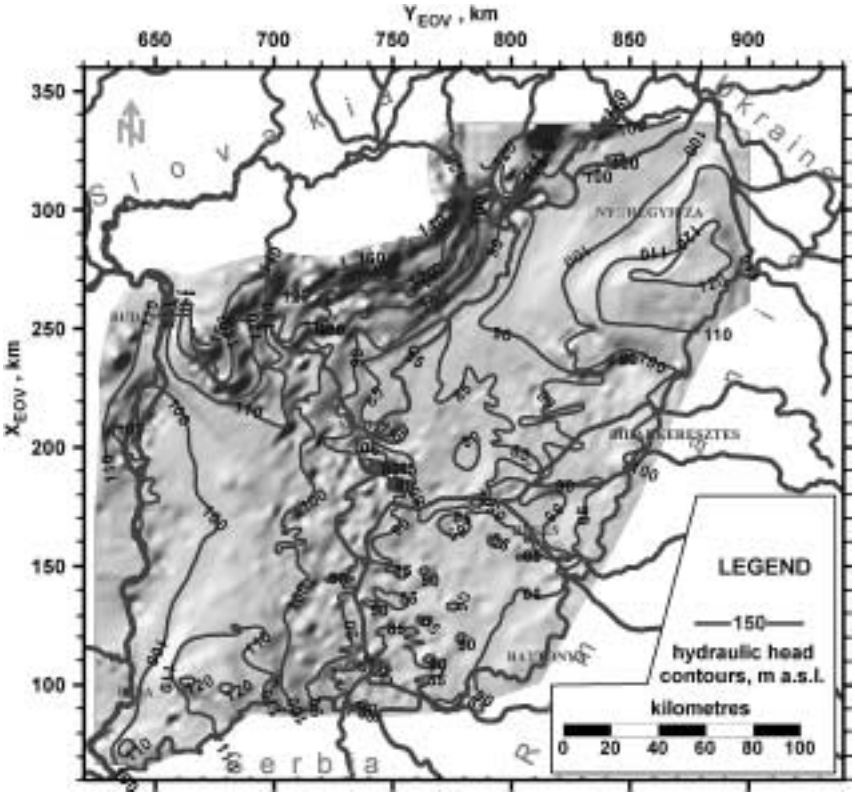

Fig. 16. Tomographic fluid potential map, $h_{1,3}$, based on 2547 measurement points in the elevation range of −100 to −300 m a.s.l.

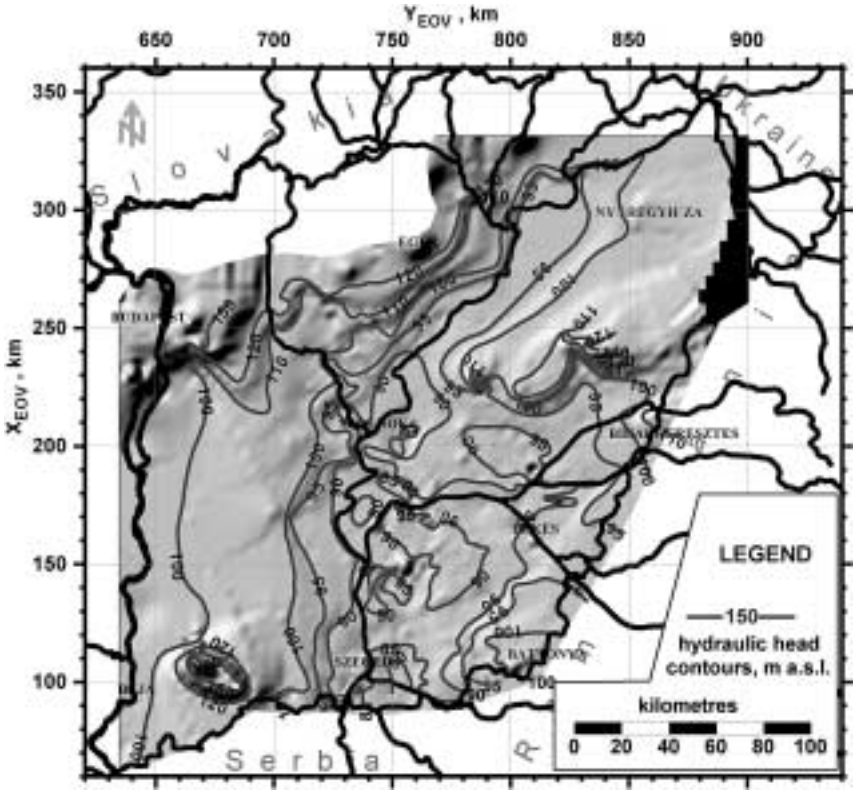

Fig. 17. Tomographic fluid potential map, $h_{3,6}$, based on 891 measurement points in the elevation range of − 300 to − 600 m a.s.l.

$i = -100$ m $\geq z \geq -300$ m $= j$ slab ($h_{1,3}$ map, Fig. 16), but abruptly reverse and increase to over 200 m in the $i = -300$ m $\geq z \geq -600$ m $= j$ slice ($h_{3,6}$ map, Fig. 17). Depending partly on the specific position of available data points, the head value of $h \approx 200$ m is maintained within the region at slightly varying locations and gradually increasing areal extent, through the maps of $h_{3,6}$ (Fig. 17), $h_{6,10}$ (not shown) and $h_{10,15}$ (Fig. 18), to the level of $z \approx -1500$ m. Although no more data are available at greater depths within the block in question, the observed values of $h > 1000$ m further east along Section H_1–H_1' (Fig. 2) suggest that the trend of downward increasing potential continues.

Three strikingly strong 'overpressure islands' can be observed on map $h_{10,15}$ (Fig. 18): (i) at Szolnok, in EOV block $X_{EOV} = 180$–200 km, $Y_{EOV} = 720$–760 km, a mound–shaped high, with $h > 200$ m; (ii) near Biharkeresztes, in EOV block $X_{EOV} = 180$–220 km, $Y_{EOV} = 800$–860 km, an elongated potential ridge, with h values exceeding 500 and 800 m; and (iii) near Battonya, in EOV block $X_{EOV} = 100$–140 km, $Y_{EOV} = 780$–800 km, with $h > 300$ m. On map $h_{15,19}$ (not shown), the mounds mentioned in (i) and (ii) nearly coalesce and h values in excess of 1000 m are common. In addition to the appearance of a growing number of overpressure islands of increasing magnitudes, an arcuate spatial arrangement in their positions also is faintly taking place. Thus the overpressure anomalies seem to be located along a slightly curved trajectory approximately following the coordinate positions of: $X_{EOV}/Y_{EOV} = 90/720$; $X_{EOV}/Y_{EOV} = 130/680$; $X_{EOV}/Y_{EOV} = 190/730$; $X_{EOV}/Y_{EOV} = 200/820$; and $X_{EOV}/Y_{EOV} = 190/860$. Between this arch of high overpressures and the island at Battonya, a potential basin seems to exist with values generally below 100 m, in the rock slab at $i = -1000$ m $\geq z \geq -1500$ m $= j$.

The foreshadowed potential arch has developed fully in the rock slab $i = -2200$ m $\geq z \geq -2500$ m $= j$ (Fig. 19), dividing the entire area into a strongly overpressured 'highland' to the west and north–west, with h values generally above 1000 m and exceeding 2000 m in places, and a relatively mildly overpressured 'potential basin' with h values, on average, between 150 and 200 m on the east and south–east side. However, within this general basin, two subbasins also appear with $h < 100$ m, while the mound at Battonya has grown to $h > 2000$ m. Also, all segments of the arcuate belt of the 'pressure escarpment' have migrated towards the centre with increasing depth, i.e. to the east, south–east and south, thereby shrinking the 'fluid potential basin's' areal extent from the higher level of $h_{10,15}$ (Figs 18 and 19, respectively).

The trend of downward rapidly increasing hydraulic head values continues to the deepest rock slab for which data are available (Fig. 14; Table 1). Observed head values reach and regularly exceed 3000 m at the elevation range of $i = -2500$ m $\geq z \geq -2800$ m $= j$, and below. However, the

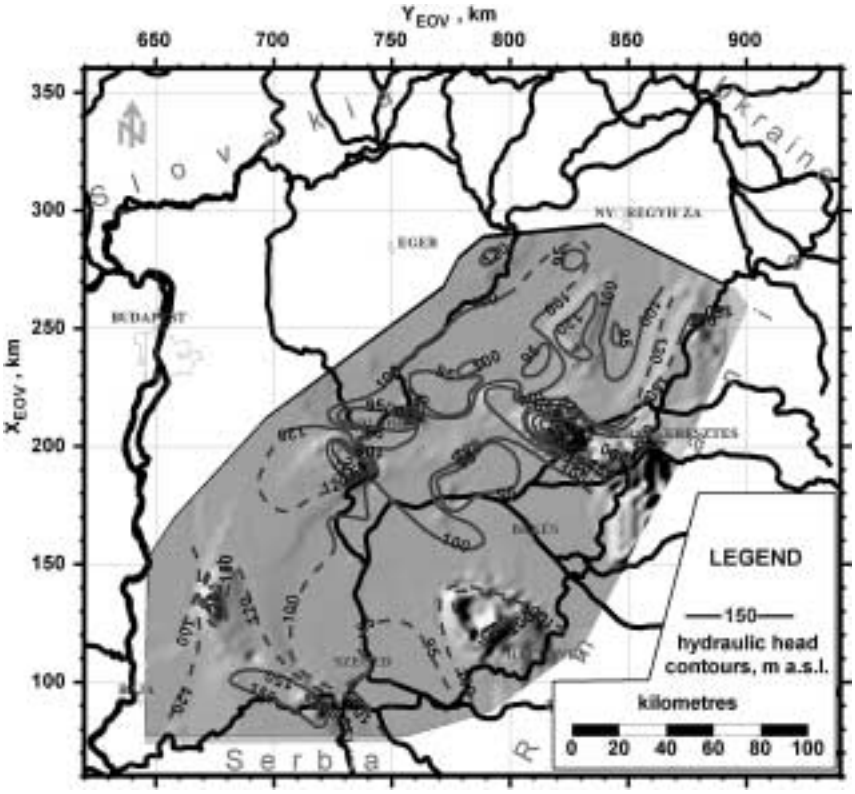

Fig. 18. Tomographic fluid potential map, $h_{10,15}$, based on 339 measurement points in the elevation range of − 1000 to − 1500 m a.s.l.

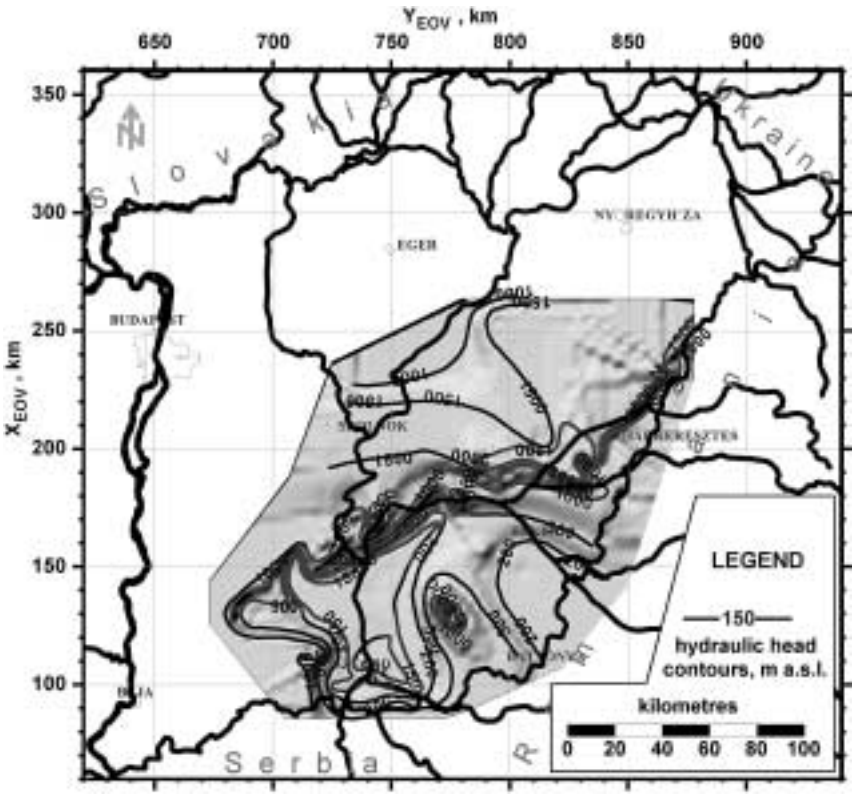

Fig. 19. Tomographic fluid potential map, $h_{22,25}$, based on 196 measurement points in the elevation range of − 2200 to − 2500 m a.s.l.

data point distribution below $z = -2800$ m is insufficient for the evaluation of pressure field patterns.

Summary

In summary, the following observations and inferences have been made from the 13 hydraulic head maps, including eight not discussed here but reported elsewhere (Tóth & Almási 1998).

(1) The fluid potential surfaces closely mimic the topographic relief between the land surface and elevation $z = -300$ m, i.e. to a depth of $\approx$ 380–480 m below land surface.

(2) Hydraulic head values decrease uniformly with depth beneath regions of topographic elevations above 100–110 m; they remain constant in areas of $\approx$ 100–110 m and rise in areas of lower elevation, down to a depth of at least $z = -300$ m.

(3) The potentiometric surface's regional configuration resembles the topography still in the elevation range of $i = -300$ m $\geq z \geq -600$ m $= j$, but 'overpressure mounds' appear beneath Illancs and Battonya, and in the middle of segment $H_3'-H_3''$ of the hydraulic section H_3-H_3'' (not shown).

(4) The 'overpressure mounds' intensify, extend, multiply and migrate in the range of $i = -600$ m $\geq z \geq -1500$ m $= j$; a 'fluid potential plateau' and a 'fluid potential basin' begin to appear on the map of $h_{10,15}$.

(5) The gradually evolving 'fluid potential plateau', to the west and north–west, and the 'fluid potential basin', to the east and south–east, are firmly established with depth down to the elevation range of $i = -2200$ m $\geq z \geq -2500$ m $= j$; they are separated by a steep 'potential escarpment'. The 'escarpment' runs through the centre of the study area striking NE–SW, with a turn to the south, west of the Tisza River, and has several lobate protrusions and embayments subnormal to its general direction.

(6) The fluid driving forces are orientated from the basement highs (horsts) to the sediment–filled troughs (grabens).

(7) Sporadic data, available for lower levels of the rock framework, indicate a continuing increase of fluid potentials with increasing depth, with values exceeding $h = 3000$ m at the elevation range of $i = -2900$ m $\geq z \geq -3500$ m $= j$.

(8) The strike direction of the main potential escarpment, and the location and direction of its embayments and lobes, appear to correlate with the principal faults in the basement and/or the Neogene basin fill (Fig. 6).

(9) Two vertically superposed pore pressure regimes can be distinguished in the area using tomographic fluid potential maps: a gravity-driven, unconfined upper regime, and a strongly overpressured lower regime.

(10) The source of the fluid driving force in the lower regime is attributed to currently active tectonic compression (argument presented later).

(11) The general sense of vertical flow in the confined regime is ubiquitously and unequivocally upwards.

(12) The principal pathways of upward flow in the confined regime are faults, fracture zones and lithologic discontinuities.

Hydraulic cross-sections, $h(z,l)$

A hydraulic cross-section is a contour line representation of the subsurface hydraulic head distribution in a vertical plane of arbitrarily chosen azimuth. In the section, h is the hydraulic head, z is the elevation referenced to sea level and l is the section's horizontal direction, or azimuth.

Four sections of a total length of approximately 850 km were constructed and evaluated for the present work, namely: $H_1-H_1'-H_1''$, $\approx$ 180 km; $H_2-H_2'H_2''$, $\approx$ 220 km; $H_3-H_3'-H_3''$, $\approx$ 300 km; and $H_4-H_4'-H_4''$, $\approx$ 150 km; or, for short reference: H_1, H_2, H_3 and H_4, respectively (Fig. 2). Because of space limitations, only sections H_1, H_2 and H_4 are displayed (Figs 20, 21 and 22). The contours of the sections are based on hydraulic head values produced in two different ways. First, point values calculated for water wells and hydrocarbon wells found within 2.0 km from either side of the sections' trace were projected horizontally onto the sections. Second, contour values of the tomographic potential maps were transferred to the proper elevation intervals of the cross-sections at the locations where the sections intersected the maps' contour lines. The technique introduces some uncertainty to the exact vertical position of the contour lines within the elevation intervals of the maps, but it provides constrained values of head in regions where otherwise none might be available.

The hydraulic cross-sections confirm and render the earlier conclusion plausible, namely that groundwater flow in the upper zones of the basin is gravity driven and regionally unconfined. In these zones, hydraulic heads decline with increasing depth under high terrains, indicating downward flow of infiltrating meteoric water. The depth of the zone of downward drive varies strongly, depending on the relief of the land surface, but probably also on the local hydrostratigraphy and the degree of interference from the deeper, overpressured regime. For instance, the depth of the potential inversion (reversal of downward drive into upward drive along a vertical) is $\approx$ 850 m at km 16 of Section H_1 (Fig. 20), but it is only $\approx$ 200 m along km 28–35. The effect of high topography is felt to a depth of $\approx$ 1700 m (elevation ≈ -1500 m) beneath the Gödöllő Hills at km 11 of H_2 (Figs 2, 21), but this depth decreases to $\approx$ 600 m under lower elevations at km 63. Further south–east on the east flank of the Duna–Tisza interfluve and beneath the plains of the Tisza and the Körös River system, fluid drive is upward at all depths. An apparent lack of a fluid potential inversion at the north end of H_4 (Fig. 22) can be explained by the termination of the section in the regions of lateral and ascending

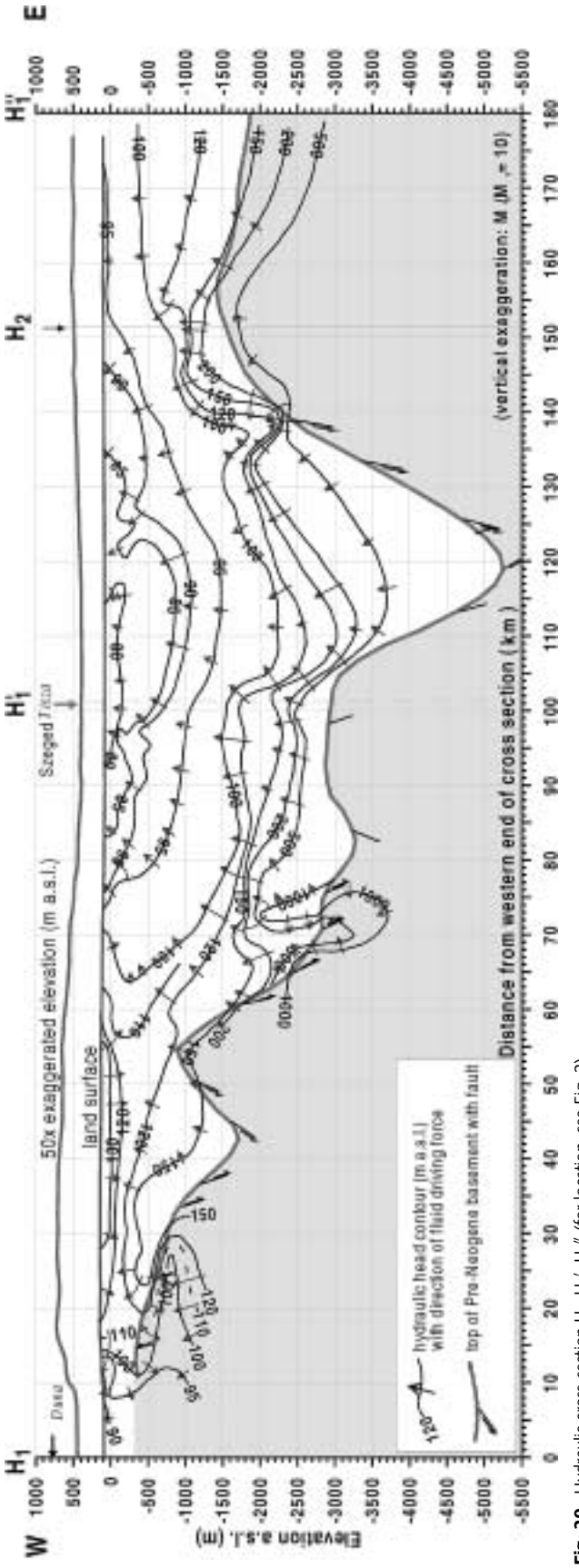

Fig. 20. Hydraulic cross-section H_1–H_1'–H_1'' (for location, see Fig. 2).

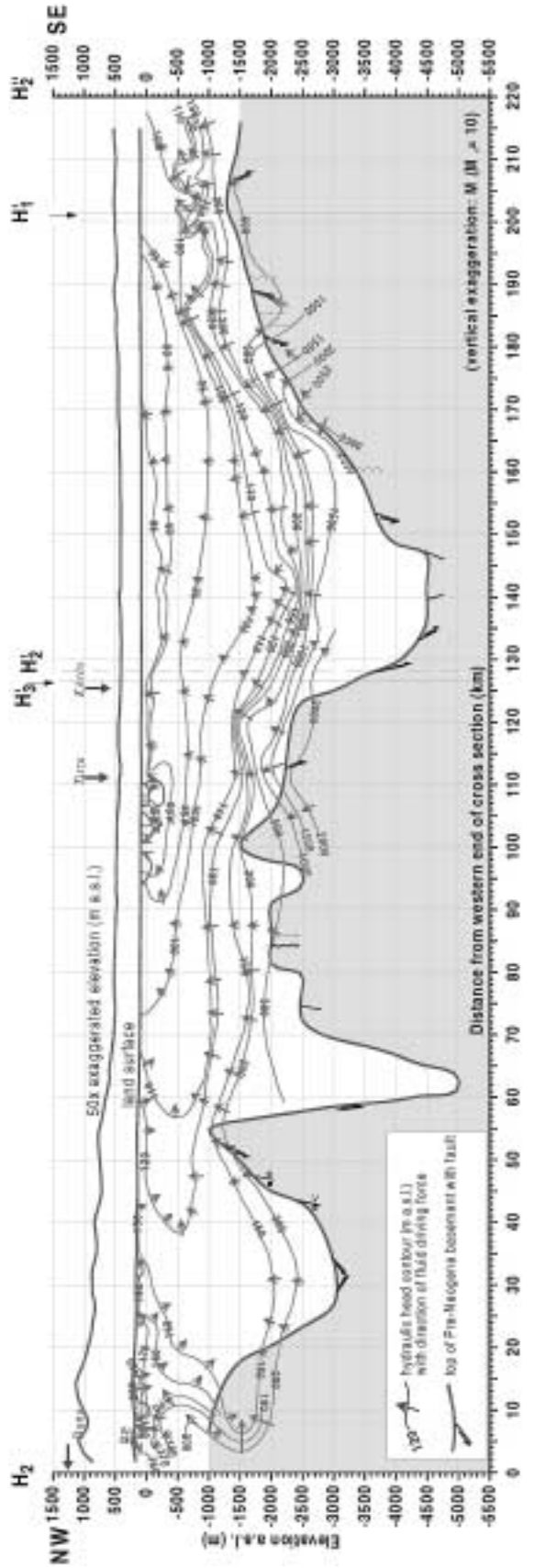

Fig. 21. Hydraulic cross-section H_2–H_2'–H_2'' (for location, see Fig. 2).

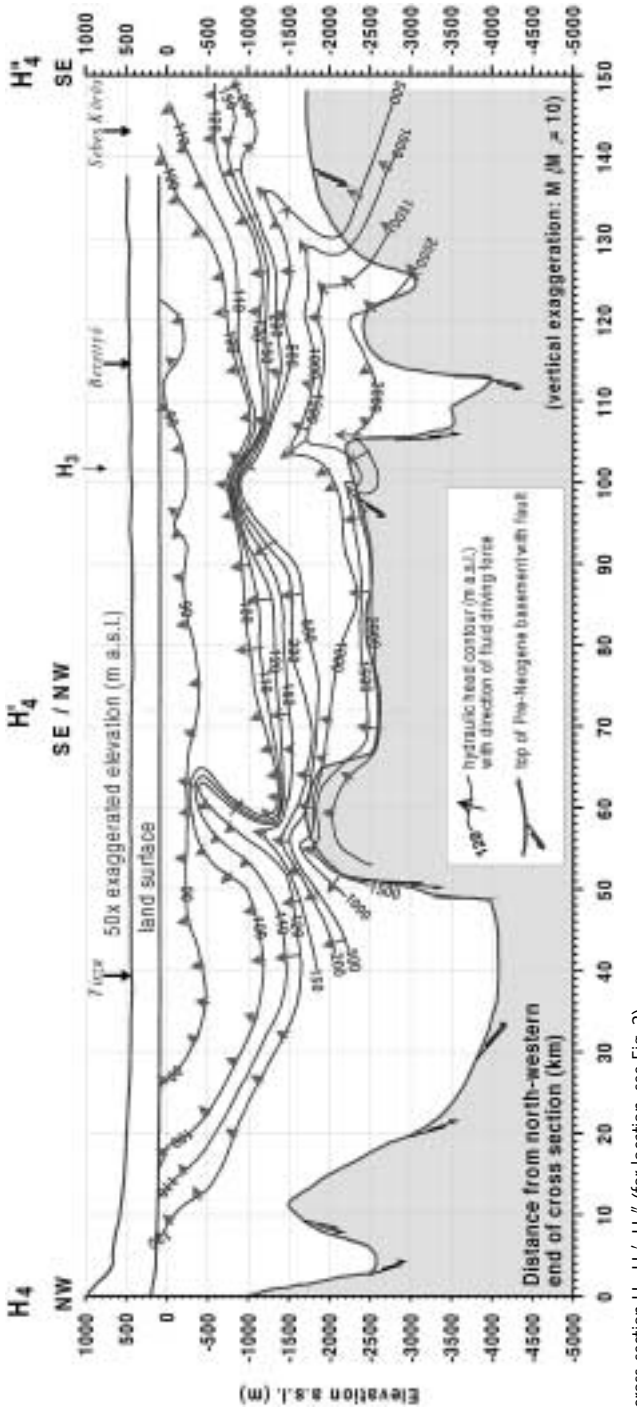

Fig. 22. Hydraulic cross-section H_4–H_4'–H_4'' (for location, see Fig. 2).

flow, i.e. short of the recharge areas of the North Central Range further north (Fig. 2).

The presence of strong overpressures is clearly recognizable beneath the gravity-driven regime on all hydraulic sections. A noteworthy property of the hydraulic head pattern in this zone is that the high-value contours mimic the undulations of the Pre-Neogene basement surface with dampened or magnified amplitudes. In general, attenuation is linked to deep, sediment-filled troughs and subbasins, whereas amplification is linked to the tops or steep flanks of the horsts. One feature of the potential pattern is striking: maximum overpressures tend to be associated with promontories of the Pre-Neogene basement. Fluid driving forces thus seem to be orientated generally from basement highs towards basement depressions. This force pattern is manifest in upward convex bands of higher valued and densely spaced contour lines running atop basement highs, while lower valued, upward concave h contours spread out widely in the deep, sediment-filled depressions.

These relations are well exemplified on Section H_1 by the basins located at km 40–45 and 110–130, and by the basement highs at km 55 and 155 (Fig. 20); on Section H_2 by the basins at km 25–40 and 135–155 and the sharp basement shoulder at km 120–125 (Fig. 21); and on Section H_4 by the prominent rounded ridge at km 52–64 (Fig. 22).

The dynamic character and geometry of the transition between the confined and unconfined hydraulic regimes depend on the local topography and the local geological conditions. The change from the high-energy lower regime to the overlying low-energy unconfined one can be gradual or stepwise. In the case of a gradual transition, the differences in the hydraulic heads between the lower and the upper zone are distributed more or less evenly over vertical distances of hundreds of metres. On the other hand, at places of stepwise transition, the change in hydraulic heads occurs within a short depth interval. The vertical hydraulic sections show that the gradual-type transitions occur mainly in the deep, sediment-filled basins as, for instance, in H_1 at km 45 and 120 (Fig. 20); in H_2 at km 30 (Fig. 21); and in H_4 at km 40 (Fig. 22). On the other hand, stepwise changes are associated primarily with basement highs or their steep flanks, e.g. in H_1 at km 145 (Fig. 20); in H_2 at km 110–120 and 170 (Fig. 21); and in H_4 at km 60 and 115–120 (Fig. 22). A possible interpretation of the cause of the stepwise transition is that the source of overpressure is nearby. Other possible factors, independent from the energy source's proximity, could be the hydrostratigraphy and tectonic structure. The stepwise character of the potential field transition may be enhanced by increased hydraulic resistance of low-permeability strata.

The possible role of faults in linking the two pressure regimes cannot be easily generalized because it depends on too many factors, the collective effects of which can rarely be evaluated. Such factors include the permeability of the fault walls and of the fault gouge, the relative position of aquitards and aquifers on opposite sides of the fault planes, the angle between the fault plane and the fluid driving forces, and the spatial and temporal variations of all these factors within the fault zone (Bjørlykke 1996; Matthäi & Roberts 1996; Yassir & Otto 1997). Nevertheless, fault zones appear to be important avenues for pressure diffusion, and thus for fluid flow, in many parts of the Great Plain Basin. This conclusion is based on numerous situations of observed spatial coincidence of fault zones with 'pressure plumes' and 'pressure ridges' along the sections as, for instance: in H1 at km 72–76, 99–104 and 138–145 (Fig. 20); in H_2 at km 182–188 and 205–206 (Fig. 21); and in H_4 at km 52–58 and 102–103 (Fig. 22). It is corroborated also by estimated vertical migration distances of hydrocarbon gases on the order of 3500 m (Clayton *et al.* 1990).

Summary

In summary, the following observations and inferences have been made from the four hydraulic cross-sections, including one not discussed here but reported elsewhere (Tóth & Almási 1998).

(1) Two principal pore pressure zones are recognized: (i) an upper, gravity-driven, unconfined zone; and (ii) a lower, overpressured, confined zone.

(2) In the overpressured zone, the flow's vertical component is uniformly upwards.

(3) The depth of the boundary between the upper and lower zones varies between 200 and 1700 m.

(4) A lower boundary of the gravity-driven flow systems cannot be identified from hydraulic observations in regional discharge areas because there the driving forces are orientated similarly to, and merge with, those of the ascending depth waters.

(5) The transition between the potential fields of the unconfined and confined zones may be gradual or stepwise abrupt.

(6) Gradual transition is prevalent in the deep, sediment-filled basins and troughs; stepwise changes are associated with basement highs and their flanks.

(7) The hydraulic head contours mimic the undulations of the Pre-Neogene basement, with reduced amplitudes in the deep, sediment-filled basins, and with amplification over the tops and steep sides of the basement ridges.

(8) In general, the lateral components of the fluid driving forces are orientated from the basement highs towards the intervening depressions.

(9) Faults and fracture zones appear to be preferential pathways for pressure diffusion, and thus fluid flow, upwards.

DISCUSSION

The most striking general feature of the basin's fluid potential field is the two domain-wide and vertically superimposed

hydraulic regimes, namely an upper, normally pressured regime and a lower, strongly overpressured regime. The departures of hydraulic heads from hydrostatic values in the upper regime are mild and consistent with topographic effects, as can be readily observed in the $p(z)$ profiles and $h(z,l)$ sections (Figs 9–13 and 20–22, respectively). In this regime, water is driven downwards under topographic highs, laterally under mid-elevations, and up towards the land surface beneath depressions. In the lower regime, the vertical component of the driving force is upwards everywhere. Consequently, the boundary between the two regimes is easily distinguished where their forces are oppositely directed, i.e. under the highlands, but it vanishes under the topographic depressions where the water is driven upwards in both regimes.

The $h_{ij}(x,y)$ and $h(z,l)$ contours show both regional trends and local perturbations in both regimes. (Note that 'local' may mean several kilometres laterally and hundreds of metres vertically on the scale of presentation.) The regional trends are manifest in the potential maps and cross-sections by h contour configurations that reflect the effect of the topography in the shallow regime, and are generally congruent, although with dampened amplitudes, with the basement's relief in the overpressured regime. In the $p(z)$ profiles, the sensitivity of the vertical pressure gradients to topographic elevations in the shallow regime is a general feature and reflects that regime's unconfined character. On the other hand, the gradients, which increase monotonically with depth in the overpressured zone, are suggestive of an energy source in or below the Pre-Neogene basement.

The local perturbations of the $h_{ij}(x,y)$ and $h(z,l)$ contours are interpreted to reflect inhomogeneities of permeability due to sedimentological or structural discontinuities. No meaningful local perturbations can be observed in the upper segments of the $p(z)$ profiles, owing probably to scaling factors. The broad scatter of pressure values in the lower segments is, on the other hand, interpreted as perturbations, and indicates lithologic heterogeneities, albeit in a lumped rather than distributed, and thus site-specific, manner.

The gravity-driven hydraulic regime

The special characteristics of the gravity-driven hydraulic regime are the hierarchically nested distribution of flow systems and the highly variable depth of the regime.

Some examples to illustrate the first point are: segments 40–95 km on hydraulic cross-section H_1 (Fig. 20), and 40 km and 90–115 km on H_2 (Fig. 21). In the first example, the recharge and discharge areas of a 55 km long flow system are superposed on a generally upward orientated flow domain, while in the second case several systems less than 10 km in lateral dimension are 'hydraulically perched' by upward flows of larger systems. The hierarchical arrangement continues upwards to systems less than 100 m in length as noted elsewhere (Angelus 1996; Arday 1996; Erdélyi 1976), but which are not discernible at the present scale. These systems are generated by small local undulations of the water table, which follows the topographic relief within a few metres, due to the generally adequate precipitation.

The strongly variable depth of the gravity-driven regime is the result of hydraulic interaction between the topographic relief, lithologic heterogeneities and overpressures in the lower hydraulic regime. In general, the gravitational regime appears deeper above the deep, sediment-filled basins and grabens (e.g. km 100–125, Section H_1, Fig. 20; km 20–40, Section H_2, Fig. 21; and km 55–60 and 130–150, Section H_4, Fig. 22). Based on the $p(z)$ profiles and cross-sections, this depth appears to vary between 200 and 1700 m.

The overpressured regime

The main observable characteristics of the overpressured regime are: ubiquitously upward orientated forces; vertical pressure gradients increasing monotonically downwards without noticeable reversals; general congruence of high hydraulic heads with the basement highs; and broad, band-like scatter of pressure values on the $p(z)$ profiles. The monotonic increase of the pressure gradients is suggestive of a source depth beneath the observational domain, while the congruence of hydraulic head maxima and basement highs indicates driving forces orientated outwards from the crystalline basement and into the sedimentary basin fills. These properties of the fluid potential field are interpreted here as coherent symptoms of a currently active, high-pressure energy source seated in the Pre-Neogene basement or beneath it.

Regarding the locus of the source of high pressures and the possible role of faults and fracture zones in causing the wide scatter of pressure values at given depths, this interpretation is corroborated by the numerical experiments of Matthäi & Roberts (1996) (Fig. 23). The experiments show the pressure and flow fields generated through the overpressured basal boundary of the flow domain in a stratified and faulted rock body to display properties similar to those observed in the Great Plain. Opposite considerations, represented by models of compaction-generated force fields, i.e. by energy sources higher up in the flow domain, tend to support the inference concerning the depth of the energy source. Such energy sources have been shown to induce overpressures which also have a downward drive, as illustrated conceptually in Neuzil (1995; Fig. 5), and by numerical models of the Gulf Coast (Harrison & Summa 1991; Fig. 15) and the Sacramento Basin, California (McPherson & Garven 1999, Fig. 12).

The other important question arising from these observations concerns the mechanism of overpressure generation. The clue to this question is sought in a genetic relation between the pore pressure field and the current state of tectonic stresses and crustal displacements in the region. As indicated by the geometric patterns of the fields of hydraulic

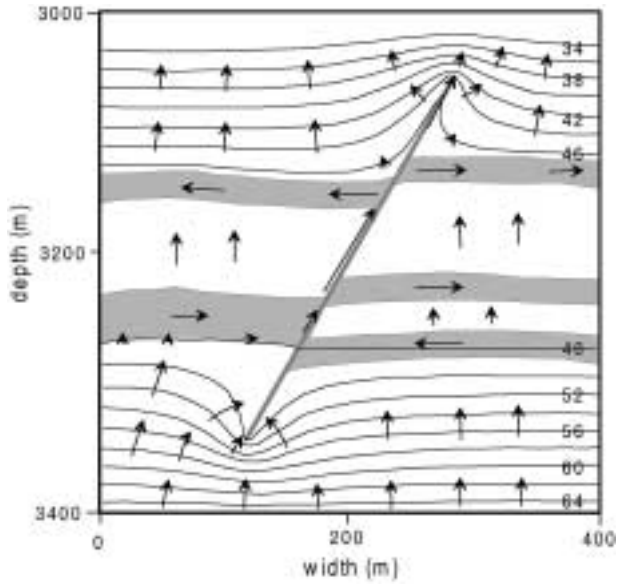

Fig. 23. Modelled fluid pressure isobars (contours in MPa) and directions of fluid flow (arrows), generated by a pressure source at the domain's base, in the vicinity of a conductive fault with displaced aquifers on opposite sides in a low-permeability environment. Pressure from surface to 3000 m depth is hydrostatic; at 3400 m it is 0.8 × lithostatic. Pressure is at steady state (adapted from Matthäi & Roberts 1996, fig. 4, with the permission of the American Association of Petroleum Geologists).

head and pore pressure in the overpressured zone, flow is out of the crystalline basement and into the adjacent or overlying clastic sediments. If this observation is combined with the structural geological and seismic evidence of a compressional stress field (Csontos 1995; Gerner *et al.* 1997; Horváth & Cloetingh 1996; Peresson & Decker 1997) as epitomized by Fig. 4 (Bada *et al.* 1998), and with the high rates of measured convergence of intraplate segments towards the study area (between 2 and 4 mm year^{-1}, Fig. 5; Grenerczy *et al.* 2001), it is tempting to ascribe the origin of overpressuring to tectonic compression. It is probably meaningful also to compare these results with the numerical experiments of McPherson & Garven (1999), who found that a crustal shortening of 2.9–3.5 mm year^{-1} can generate 10–15 MPa overpressures at a depth of 3000 m in the Sacramento Basin of California. They observed further that localized regions of higher compressibility or lower permeability could produce local overpressures greater than 25 MPa even at shallower depths, results that are quite consistent with the empirical findings of the present study.

The question may nevertheless be asked if the permeabilities accepted for the Great Plain Basin's rocks are not too high to maintain the observed disequilibrium (over) pressures. The answer is: the observed facts suggest apparently not. In theory, this question can be explored quantitatively by means of Neuzil's (1995) concept of 'geological forcing'. In practice, however, the uncertainties in estimating the values of parameters, such as the volumetric strain rate as derived from linear strain rates (e.g. Fig. 5), or the characteristic flow length or effective basin size (which are required to calculate the strength of forcing, compression in the present case, or the rocks' hydraulic resistance), would render the results indefensible. Instead, another observation by Neuzil (1994) might be invoked to resolve the apparent dichotomy of the coexistence of high permeabilities and high overpressures. Neuzil (1994; p. 149) observed that, owing to their relatively permeable subunits, argillaceous formations can be much less permeable than the values obtained from their large-scale mapping. This observation might be applicable to the available permeability values for the rock framework of the Hungarian Great Plain. High-permeability discontinuities due to faults, fracture zones and sedimentary windows are well known in the basin's rock framework (e.g. Figs 7 and 8), as well as clearly manifest by high values of hydraulic head anomalies on the potential maps (Figs 17–19) and cross-sections (Figs 20–22). In addition, the major geothermal anomalies in the area can be interpreted as indications of localized ascent of deep-seated hot formation waters (Alföldi *et al.* 1978; Lenkey 1993).

Whereas the observed distributions of pore pressures, hydraulic heads, lithologic properties and crustal movements are consistent in suggesting tectonic compression as the principal source of overpressuring in the Great Plain of Hungary, other potential mechanisms are unlikely to contribute significantly.

As mentioned before, compaction would drive fluids from the centres of the grabens towards the horsts; in reality, the opposite is true. Also, no significant downward component of the driving force seems to exist, and the region of major overpressuring is in the most highly consolidated, i.e. least compressible, older rocks of the basement, rather than in the more highly deformable, younger and partially consolidated basin fill.

Volumetric expansion of maturing hydrocarbons is an unlikely source of overpressures in the area. According to Szalay & Koncz (1993; p. 305): 'The deep basin sediments along the axis of the deep troughs presently are in the main phase of dry gas or wet gas generation.' Yet, as is clearly observable on the hydraulic cross-sections (Figs 20–22), the horizontal components of the driving forces point in all cases from the basement highs towards the basin centres, i.e. towards the loci of hydrocarbon maturation.

Osmosis must also be ruled out as a potential source of overpressures because of the inadequate salinity contrasts in the formation waters, and the insufficient thickness, areal continuity and too high permeabilities of potential shale membranes. According to Neuzil (2000; Fig. 3), the maximum osmotic pressure that could be generated in the highly continuous and argillaceous Pierre Shale of central South Dakota, USA (k = 10^{-6}–10^{-5} md) is approximately 0.4 MPa at a depth of 3 km, if a porosity of 0.2 and total dissolved solids content (TDS) contrast of 3 g L^{-1} are assumed. This

value is nearly two orders of magnitude less than that observed in the Great Plain Basin.

In the case of aquathermal pressuring, the loci of maximum overpressures would be expected to coincide with the basin's deepest and hottest subsiding centre. Also, vertical pressure gradients should be nearly hydrostatic in the overpressured compartments below the top seals. Neither of these situations can be observed.

The buoyancy of light fluids (hydrocarbon gases, CO_2, oil) would produce overpressures orders of magnitudes less, as well as vertical pressure gradients noticeably less, than hydrostatic. Furthermore, overpressures are ubiquitous in the basin while the required fluids occur sporadically.

The transitional zone

Perhaps the most significant characteristics of the zone of transition between the overpressured and normally pressured hydraulic regimes are its widely variable depth and the lack of an identifiable single controlling factor. The depth and location of the transition can be determined on the $p(z)$ profiles in a given geographical region by the depth of the break in the gradients away from the hydrostatic line towards higher values; by the location and depth on the $h_{ij}(x,y)$ maps where superhydrostatic pressures appear; and by the location and depth of bands of congested contour lines on the $h(z,l)$ cross-sections. The wide variation in depth is immediately evident, and the lack of either a lithologic or stratigraphic control was pointed out in connection with the analysis of the $p(z)$ profiles. Structural discontinuities, such as faults and fracture zones, and probably also high-permeability sedimentary windows, are avenues of hydraulic pressure dissipation and fluid migration from the overpressured regime to the gravity-driven zone. In addition to the structurally controlled interfingering type of transition, diffusion also must occur across the formations due to the high vertical gradients and relatively high matrix permeabilities.

CONCLUSIONS

This paper presents a summary of the characteristics and interpretation of the observed subsurface fluid potential patterns in the Hungarian Great Plain region of the Pannonian Basin located in Central Europe. The study area proper covers approximately 40 000 km^2 at a topographic elevation range of $\approx$ 80–200 m and is surrounded by the almost closed ring of the Alps, Carpathians and Dinarides. In the area, thick semi- to unconsolidated clastics of marine, deltaic, lacustrine, fluviatile and eolian sediments of Neogene age rest on a Pre-Neogene basement of brittle flysch, carbonate and metamorphic rocks of high relief with a horst-and-graben topography. After a period of crustal extension and rifting, a tectonic reversal to a compressional stress regime started in the Late Miocene. It is still ongoing, as indicated by structural, geological and geophysical observations, as well as recent satellite geodetical measurements.

The basin hydrostratigraphy has been divided into five regionally extensive major units, namely the Pre-Pannonian (k = 100 md), Szolnok (k = 10–100 md) and Great Plain (k = 1000 md) Aquifers, and the Endrőd (k = 0.1–10 md) and Algyő (k = 1–10 md) Aquitards. The Algyő Aquitard contains many high-permeability lenses, and both aquitards are dissected by numerous faults and fractures.

Characterization of the fluid potential field is based on 16 192 hydraulic head values culled from more than 52 000 water level and pore pressure measurements conducted in shallow dug wells, drilled water wells up to 1500 m deep and hydrocarbon wells reaching depths exceeding 4000 m. The data were processed by three different techniques of representation: vertical pressure-elevation profiles, $p(z)$; tomographic hydraulic head maps, $h_{ij}(x,y)$; and vertical hydraulic head cross-sections, $h(z,l)$.

The observed fluid potential patterns show two superimposed and laterally extensive hydraulic regimes in the basin with independent and separate sources of fluid drives. The top regime is gravity driven, regionally unconfined, normally pressured and is recharged from precipitation. Its depth varies from 200 to 1700 m. The lower regime is strongly overpressured (hydraulic heads may exceed 2500 m locally) with vertical gradients increasing monotonically with depth, regionally confined, and thought to be overpressured by tectonic compression of the basement. The main sites of overpressure are the basement's horsts, from which divergent fluid impelling forces are orientated upwards and towards the interhorst basins and grabens. Communication between the two pressure regimes occurs by diffusion across geological strata and/or through high-permeability structural and sedimentological discrete discontinuities. The different methods and avenues of cross-formational communication result in vertical interfingering of the two regimes with a transitional zone varying between 200 and 1700 m in depth. Some of the high-permeability avenues for pressure dissipation and fluid flow are manifest by perturbations of the potential field. These perturbations provide diagnostic patterns that may be of practical value for water resources development and petroleum and geothermal exploration.

ACKNOWLEDGEMENTS

Subsurface data for the work reported in this paper were provided by MOL Rt. (Hungarian Oil and Gas Co., Ltd) and, through Dr Judit Szőnyi, by the Department of Applied and Environmental Geology, Eötvös Loránd University of Science (ELTE), both of Budapest, Hungary. We appreciate the personal interest and support of Dr István Bérczi, and are grateful for the technical and scientific advice, logistical assistance, continual colleagueship and personal friendship received from Mr Sándor Pap and Dr István Révész, all of

MOL Rt. Particular thanks are due to Mr Gy. Grenerczy of ELTE and the Hungarian Satellite Observatory for permitting the use of the intraplate velocity map (Fig. 5) prior to publication in their own paper. The present version of the work benefitted greatly from penetrating comments and suggestions by Drs Grant Garven and Mark Person. The 3 year long project was made possible by financial contributions and logistical support from MOL Rt., and Research Grant No. A-8504 from the Natural Sciences and Engineering Research Council of Canada (NSERC) to the first author.

REFERENCES

Alföldi L, Erdélyi M, Gálfi J, Korim K, Liebe P (1978) A geothermal flow system in the Pannonian Basin: case history of a complex hydrogeological study at Tiszakécske. In: *Hydrogeology of Great Sedimentary Basins* (ed. Rónai A), pp. 716–32. Hungarian Geological Institute, Mémoires XI, Budapest.

Angelus B (1996) A felszínalatti vizáramlások tanulmányozása a Duna–Tisza köze középsö területén, Foktő és Csánytelek között [Study of the groundwater flow systems in the central region of the Duna–Tisza interfluve, between the towns of Foktő and Csánytelek]. MSc Thesis, Eötvös Loránd University, Budapest, Hungary (in Hungarian).

Arday A (1996) A felszínalatti vizáramlások tanulmányozása a Duna–Tisza köze déli részén [Study of the groundwater flow systems in the southern region of the Duna–Tisza interfluve]. MSc Thesis, Eötvös Loránd University, Budapest, Hungary (in Hungarian).

Bada G, Cloetingh S, Gerner P, Horváth F (1998) Sources of recent tectonic stress in the Pannonian region; inferences from finite element modelling. *Geophysical Journal International*, **134**, 87–101.

Ballentine CJ, O'Nions RK, Oxburgh ER, Horváth F, Deák J (1991) Rare gas constraints on hydrocarbon accumulation, crustal degassing and groundwater flow in the Pannonian Basin. *Earth and Planetary Science Letters*, **105**, 229–46.

Bérczi I, Hámor G, Jámbor Á, Szentgyörgyi K (1988) Neogene sedimentation in Hungary. In: *The Pannonian Basin; a Study in Basin Evolution* (eds Royden LH, Horváth F), pp. 57–67. American Association of Petroleum Geologists — Memoir 45, Tulsa, OK.

Bérczi I, Kókai I (1976) Hydrogeological features of some deep-basins in SE-Hungary as revealed by hydrocarbon exploration. In: *Hydrogeology of Great Sedimentary Basins* (ed. Rónai A), pp. 69–93. Hungarian Geological Institute, Mémoires XI, Budapest.

Bjørlykke K (1997) Lithological control on fluid flow in sedimentary basins. In: *Fluid Flow and Transport in Rocks — Mechanisms and Effect* (eds Jamtveit B, Yardley BWD), pp. 1–14, Chapman & Hall, London.

Clayton JL, Spencer CW, Koncz I, Szalay A (1990) Origin and migration of hydrocarbon gases and carbon dioxide, Békés Basin, southeastern Hungary. *Organic Geochemistry*, **8**, 233–47.

Csontos L (1995) Tertiary tectonic evolution of the Intra-Carpathian area: a review. *Acta Vulcanologica*, **7**, 1–13.

Dobos I (1985) Exploration of subsurface waters in the Neogene basins. In: *Proceedings of Neogene Mineral Resources in the Carpathian Basin; Historical Studies on Their Utilization, VIIIth RCMNS Congress, Hungary* (ed. Hála J), pp. 531–55. Hungarian Geological Survey, Budapest.

Erdélyi M (1976) Outlines of the hydrodynamics and hydrochemistry of the Pannonian Basin. *Acta Geologica Academiae Scientiarium Hungarica*, **20**, 287–309.

Freeze RA, Witherspoon PA (1967) Theoretical analysis of regional groundwater flow. 2. Effect of water table configuration and subsurface permeability variation. *Water Resources Research*, **3**, 623–34.

Gajdos I, Pap S, Somfai A, Völgyi L (1983) Az alföldi Pannóniai (s.l.) képzõdmények litosztratigráfiai egységei [Lithostratigraphic units of the Pannonian (s.l.) in the Great Hungarian Plain]. *Magyar Állami Földtani Intézet (Hungarian Geological Survey)*, **70**, 1–70 (in Hungarian).

Gerner P, Bada G, Dövényi P, Mueller B, Oncescu MC, Cloetingh S, Horváth F (1999) Recent tectonic stress and crustal deformation in and around the Pannonian basin: data and models. In: *The Mediterranian Basins: Tertiary Extension within the Alpine Orogen* (eds Durand B, Jolivet L, Horváth F, Séranne M), pp. 269–94. Geological Society of London Special Publication, 126.

Grenerczy Gy, Kenyeres A, Fejes I (2000) Present crustal movement and strain distribution in Central Europe inferred from GPS measurements. *Journal of Geophysical Research*, **105**, 21 835–21 846.

Grenerczy Gy, Kenyeres A, Fejes I (2001) Present crustal deformation pattern in the PANCARDI region: constraints from space geodesy. In: *Neotectonics and Seismicity of the Pannonian Basin and Surrounding Orogens; a Memoir on the Pannonian Basin* (eds Cloetingh S, Horváth F, Bada G, Lankreijer A). European Geological Society Special Publication (preprint).

Halász B (1975) Rétegzett hidrológiai rendszerek sajátosságai (Properties of stratified hydrologic systems). *Hidrológiai Közlöny (Journal of the Hungarian Hydrological Society)*, **55**, 505–7.

Harrison WJ, Summa LL (1991) Paleohydrology of the Gulf of Mexico basin. *American Journal of Science*, **291**, 109–76.

Horváth F, Cloetingh S (1996) Stress-induced late-stage subsidence anomalies in the Pannonian Basin. *Tectonophysics*, **266**, 287–300.

Hubbert MK (1940) The theory of ground-water motion. *Journal of Geology*, **48**, 785–944.

Hubbert MK (1953) Entrapment of petroleum under hydrodynamic conditions. *Bulletin of the American Association of Petroleum Geologists*, **37**, 1954–2026.

Hungarian Geological Survey (1993) *Field trip C: Oil and Gas, Subsurface Water, and Geothermy in the Pannonian Basin, Excursion Guide* (eds Liebe P, Révész I). 8th Meeting of the Association of European Geological Societies, Hungary.

Juhász Gy. (1991) Lithostratigraphic and sedimentological framework of the Pannonian (s.l.) sedimentary sequence in the Hungarian Plain (Alföld), eastern Hungary. *Acta Geologica Hungarica*, **34**, 53–72.

Korim K (1966) A pannóniai rétegek váztároló- és vízadóképességét meghatározó földtani tényezõk (Geological factors determining water storage and water supply capacity of the Pannonian strata). *Hidrológiai Közlöny (Journal of the Hungarian Hydrological Society)*, **46**, 522–31.

Korim K, Liebe P (1973) A szentesi hévíztároló rendszer (The thermal water storage system of Szentes). *Vízügyi Közlemények (Hydraulic Engineering)*, **55**, 290–311.

Lenkey L (1993) A tiszakécskei hőanomália vizsgálata termikus konvekció numerikus modellezésével (Examination of the geothermal anomaly of Tiszakécske by numerical modeling of thermal convection). *Magyar Geofizika (Hungarian Geophysics)*, **34**, 30–45.

Matthäi SK, Roberts SG (1996) The influence of fault permeability on single-phase fluid flow near fault-sand intersections: results from steady-state high-resolution models of pressure-driven fluid flow. *Bulletin of the American Association of Petroleum Geologists*, **80**, 1763–79.

McPherson BJOL, Garven G (1999) Compressional tectonics, hydrodynamics and overpressure mechanisms in the Sacramento Basin, California. *American Journal of Science*, **299**, 429–66.

Neuzil CE (1994) How permeable are clays and shales? *Water Resources Research*, **30**, 145–50.

Neuzil CE (1995) Abnormal pressures as hydrodynamic phenomena. *American Journal of Science*, **295**, 742–86.

Neuzil CE (2000) Osmotic generation of 'anomalous' fluid pressures in geologic environments. *Nature*, **403**, 182–4.

Pap S (1976) Alföldi és Északi-Középhegységi kőolaj-földgáztároló kőzetek (Hydrocarbon bearing reservoir rocks of the Great Hungarian Plain and the North Hungarian Highland). *Földtani Közlöny (Bulletin of the Hungarian Geological Society)*, **106**, 555–80.

Peresson H, Decker K (1997) Far-field effects of Late Miocene subduction in the Eastern Carpathians: E–W compression and inversion of structures in the Alpine–Carpathian–Pannonian region. *Tectonics*, **16**, 38–56.

Royden LH, Horváth F (eds) (1988) *The Pannonian Basin: A Study in Basin Evolution*. American Association of Petroleum Geologists — Memoir 45, Tulsa, OK.

Rumpler J, Horváth F (1988) Some representative seismic reflection lines from the Pannonian basin and their structural interpretation. In: *The Pannonian Basin; a Study in Basin Evolution* (eds Royden LH, Horváth F), pp. 153–71. American Association of Petroleum Geologists — Memoir 45, Tulsa, OK.

Szalay Á, Koncz I (1993) Migration and accumulation of oil and gas generated from Neogene source rocks in the Hungarian part of the Pannonian Basin. In: *Generation, Accumulation and Production of Europe's Hydrocarbons III* (ed. Spencer AM), pp. 303–9. Special Publication of the European Association of Petroleum Geoscientists no. 3, Springer-Verlag, Berlin.

Szebényi L (1955) Artézi vizeink függőleges irányú mozgásáról (On the vertical motion of our artesian waters). *Hidrológiai Közlöny (Journal of the Hungarian Hydrological Society)*, **35**, 437–9.

Tóth J (1963) A theoretical analysis of groundwater flow in small drainage basins. *Journal of Geophysical Research*, **68**, 4795–812.

Tóth J (1995) Hydraulic continuity in large sedimentary basins. *Hydrogeology Journal*, **3**, 4–16.

Tóth J, Almási I (1998) Szénhidrogén kutatás az Alföldön hidrogeológiai szempontok figyelembevételével: Zárójelentés. A Magyar Olaj- és Gázipari Rt. megbízásából és számára [Hydrocarbon exploration in the Great Plain using hydrogeological principles: Final Report. Prepared for the Hungarian National Oil & Gas Company, Plc.]. University of Alberta, Edmonton, Canada (in-house report, in Hungarian).

Yassir N, Otto CJ (1997) Hydrodynamics and fault seal assessment in the Vulcan Sub-basin, Timor Sea. *Australian Petroleum Production and Exploration Association Journal*, **36**, 380–9.